



## OPEN ACCESS

## EDITED BY

Scott L. Painter,  
Oak Ridge National Laboratory (DOE),  
United States

## REVIEWED BY

Gregory Todd Carling,  
Brigham Young University, United States  
Brady Adams Flinchum,  
CSIRO Land and Water, Australia

## \*CORRESPONDENCE

Rodrigo Andrés Sánchez  
✉ andressanchez@arizona.edu

## †Deceased

## SPECIALTY SECTION

This article was submitted to  
Water and Critical Zone,  
a section of the journal  
Frontiers in Water

RECEIVED 19 January 2023

ACCEPTED 14 March 2023

PUBLISHED 02 May 2023

## CITATION

Sánchez RA, Meixner T, Roy T, Ferré PT,  
Whitaker M and Chorover J (2023) Physical and  
biogeochemical drivers of solute mobilization  
and flux through the critical zone after wildfire.  
*Front. Water* 5:1148298.  
doi: 10.3389/frwa.2023.1148298

## COPYRIGHT

© 2023 Sánchez, Meixner, Roy, Ferré, Whitaker  
and Chorover. This is an open-access article  
distributed under the terms of the [Creative Commons Attribution License \(CC BY\)](https://creativecommons.org/licenses/by/4.0/). The use,  
distribution or reproduction in other forums is  
permitted, provided the original author(s) and  
the copyright owner(s) are credited and that  
the original publication in this journal is cited, in  
accordance with accepted academic practice.  
No use, distribution or reproduction is  
permitted which does not comply with these  
terms.

# Physical and biogeochemical drivers of solute mobilization and flux through the critical zone after wildfire

Rodrigo Andrés Sánchez<sup>1,2\*</sup>, Thomas Meixner<sup>1†</sup>, Tirthankar Roy<sup>3</sup>,  
Paul Ty Ferré<sup>1</sup>, Martha Whitaker<sup>1</sup> and Jon Chorover<sup>4</sup>

<sup>1</sup>Department of Hydrology and Atmospheric Sciences, University of Arizona, Tucson, AZ, United States, <sup>2</sup>Dornsife Environmental Studies Program, University of Southern California, Los Angeles, CA, United States, <sup>3</sup>Department of Civil and Environmental Engineering, University of Nebraska-Lincoln, Lincoln, NE, United States, <sup>4</sup>Department of Environmental Science, University of Arizona, Tucson, AZ, United States

A nine-year time series of nutrient cation and anion concentration and efflux from three forested catchments in the Jemez River Basin Critical Zone Observatory (JRB-CZO) in northern New Mexico was used to quantify the pulse of chemical denudation resulting from varying levels stand-replacing wildfire intensity in May–June of 2013. The 3 years of pre-fire and 6 years of postfire data were also probed to shed light on the mechanisms underlying the pulsed release and the subsequent recovery. The initial large solute pulse released to the streams— $K^+$ ,  $Ca^{2+}$ ,  $Mg^{2+}$ ,  $SO_4^{2-}$ ,  $Cl^-$ , dissolved inorganic carbon (DIC), dissolved organic carbon (DOC), and total dissolved nitrogen (TDN)—was caused by leaching of hillslope ash deposits during the first monsoon storms post-fire. Debris flow following the wildfire likely redistributed much of the ash-containing sediments along streams and valley bottoms. Sustained elevated solute concentrations observed in the surface waters throughout the post-fire period relative to pre-fire baselines is consistent with these soluble materials being periodically flushed from the soils during wet seasons, i.e., snowmelt and summer monsoons. As microbial mediated reactions and biotic uptake—due to plant regrowth—recover after fire, nutrient ion export (e.g.,  $NO_3^-$ ,  $Cl^-$  and  $SO_4^{2-}$ ) steadily decreased toward the end of the post fire period, but remained above pre-fire levels, particularly for  $NO_3^-$  and  $SO_4^{2-}$ . Surface water concentrations of polyvalent cations (e.g., Al and Fe) decreased significantly after the fire. Our observations suggest that changes in organic matter composition after fire (e.g., increased humification index—HIX) and the presence of pyrogenic carbon may not favor organo-metal complexation and transport. Finally, differences in burn severity among the three watersheds presented in this study, provide insights of the relative impact of solute exports and resilience. The catchments that experienced high burn severity exhibited greater solute fluxes than the less severely burn. Moreover, despite these differences, toward the end of the post-fire period these surface waters presented low and similar solute effluxes, indicating system recovery. Nonetheless, magnitudes and rebounds were solute and process specific. The results of this study highlight the importance of surface and near surface physical and biogeochemical processes on the long-lasting geochemical denudation of forested catchments following wildfires of varying intensities.

## KEYWORDS

biogeochemistry, wildfires, critical zone, solute mobilization, fire severity

## Key points

- Post-fire soil physical and biogeochemical processes drive solute mobilization and exports in the Critical Zone.
- Fire severity and hydrologic regimes play an important role in catchment chemical denudation after fire.

## 1. Introduction

Wildfires in the western United States have significantly increased in number, size, and severity since 1990 (Smith et al., 2011; Potthast et al., 2017). Forested headwater catchments in semi-arid areas are prone to wildfires. Prolonged drought periods, changes in climate through increased temperatures and changed precipitation regimes, and increased fuel loads associated with fire suppression practices have made these ecosystems susceptible to catastrophic, stand-replacing high intensity wildfire events along with higher rates of overstory mortality and post-fire erosion in these water-stressed environments (Stephens et al., 2004; Goulden and Bales, 2019).

Through disruption of ecosystem water balance and element cycling, wildfires alter critical zone processes that regulate streamflow and solute concentrations downstream (Rhoades et al., 2019). Burned forested catchments impact downgradient water supply quality (Blake et al., 2009; Smith et al., 2011). Post-fire runoff, erosion, and mineral dissolution may impact solute exports in burned watersheds (Smith et al., 2011). Furthermore, the magnitude, duration and extent of downstream surface water quality changes following a wildfire may be a function of post-fire precipitation events, erosion rates, and associated transport capacity (Smith et al., 2011).

Studies that have investigated the effects of wildfires in forested watersheds have observed elevated solute effluxes post-fire (Chorover et al., 1994; Williams and Melack, 1997b; Stephens et al., 2004; Smith et al., 2011; Rust et al., 2018; Rhoades et al., 2019). Increased concentrations of major cations, i.e., Na<sup>+</sup>, K<sup>+</sup>, Ca<sup>2+</sup> and Mg<sup>2+</sup>, have been associated with transport processes from the soil to surface waters (Chorover et al., 1994). Because erosion rates and sediment yields increase after fire (Rhoades et al., 2011; Orem and Pelletier, 2016), physical transport mechanisms have been implicated in driving elevated nutrient and metal ion concentrations in surface waters of burned forested catchments; labile solutes bound to sediments are easily removed from burned soils *via* surface runoff (Rust et al., 2018). However, the precise sources of post-fire solutes, their relationship between post-fire biogeochemical processes, and the pathways of solute transport through the surface and subsurface warrants further investigation (Rust et al., 2018; Ackley et al., 2021).

Fires directly affect the uppermost soil layers, combusting surficial biomass and thereby altering solute adsorption, ion exchange, and dissolution reactions on minerals just below the surface, as well as biotic uptake and immobilization processes. These changes may drive the magnitude and persistence over time of solute concentrations in the surface waters of forested catchments prone to wildfires (Chorover et al., 1994; Williams and Melack, 1997a). Moreover, in systems with a high groundwater contribution to surface water discharge, cation and Si fluxes

may provide insights of catchment responses to environmental disturbances (Meixner et al., 2004). It has been argued that forest fires may alter hydrologic partitioning processes (Harpold et al., 2014), and that variability in stream chemical concentrations may respond to changes in surface and subsurface water flow paths—shifts in mineral weathering reactions, cation exchange and biological processes may occur as water flows through areas with different bedrock mineralogy and lithology (Meixner et al., 2004; White et al., 2019). Thus, it is imperative to couple post-fire physical and biogeochemical processes to further our understanding of the mechanisms that govern solute concentrations and exports in surface waters of burned forested watersheds in the short- and long-term.

Research on post-wildfire watershed hydrology has shown significant increases in streamflow (Kunze and Stednick, 2006; Maina and Siirila-Woodburn, 2020). These shifts are thought to be related to changes in infiltration processes (DeBano, 2000; Shakesby and Doerr, 2006; Jung et al., 2009) and/or decreased evapotranspiration due to forest defoliation (Clark et al., 2012). In snow-dominated catchments, vegetation drives snow accumulation and ablation (Musselman et al., 2008; Broxton et al., 2015), thus decreases in snow water equivalent (SWE) peaks after fires have been attributed to increases in snowpack ablation and shifts from vegetative to topographic controls on snow accumulation (Harpold et al., 2014). These shifts in snow distribution may affect post-fire snow water partitioning, impacting water routing and residence times, which may lead to increments in surface water discharge (Kunze and Stednick, 2006; Harpold et al., 2014).

In this study we compared pre- and post-fire surface water solute concentrations. We sought to assess whether the observed changes in stream chemical concentrations are responses to an alteration of the underlying biogeochemical processes. This work is focused on three headwater catchments (La Jara, Upper Jaramillo, and History Grove, Figure 1), that contribute to the East Fork of the Jemez River, and which are part of the Jemez River Basin-Critical Zone Observatory (JRB-CZO) within the Valles Caldera National Preserve (VCNP) in northern New Mexico. In 2013 the Thompson Ridge Wildfire was ignited when wind caused a tree to fall into a power line. The subsequent fire burned approximately 23,695 acres in the VCNP (Cerrato et al., 2016). Burn severity and intensity varied among these three catchments (Figure 2), and we postulated that post-fire physical and biogeochemical processes would differ accordingly.

Because of a significant pre-fire record of hydrologic and hydrochemical behavior, the Thompson Ridge Wildfire in the JRB-CZO offered a unique opportunity to understand the interaction of fire with erosion, biogeochemical, and hydrologic processes. Prior research at the site indicated that subsurface flow is the primary driver of streamflow in this system (Zapata-Rios et al., 2016; McIntosh et al., 2017; Olshansky et al., 2018b; White et al., 2019). Moreover, in a volcanic setting such as the VCNP, the complex mineralogy and subsurface architecture control routing, residence times, and geochemical evolution of water as it moves through the critical zone (White et al., 2019; Moravec et al., 2020). The acquired underlying knowledge of the system, in addition to the available pre- and post-fire solution chemistry data, shed light on the possible linkages between hydrological and biogeochemical processes on solute fluxes following wildfire. We sought to address

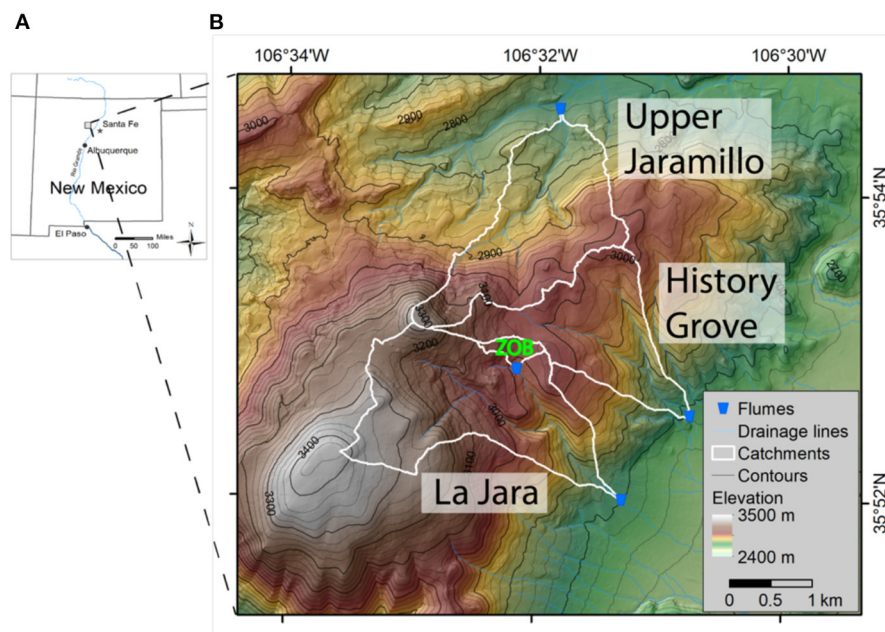


FIGURE 1

(A) The Jemez River Basin Critical Zone Observatory (JRB-CZO) located on the Valles Caldera National Preserve (VCNP) in northern New Mexico. (B) Headwaters first-order study catchments: La Jara, History Grove and Upper Jaramillo originate on different aspects around highest peak (Redondo Peak) at the VCNP. The zero-order-basin (ZOB) is nested within La Jara catchment.

the following three questions in our research: (1) *What are the patterns of solute concentrations and fluxes in response to wildfire?* (2) *What role do biogeochemical processes have in explaining these patterns?* (3) *What role do fire severity and hydrologic processes play in the amplitude and resilience of solute exports?*

We measured 3 years of pre-fire and 6 years of post-fire surface water chemistry data and stream water discharge to assess changes in the patterns of solute concentrations. We then compared pre- and post-burn solute annual fluxes and mean concentration to evaluate the possible mechanisms that drive alteration in surface water geochemistry after wildfires.

## 2. Materials and methods

### 2.1. Study area

The JRB-CZO comprises several headwater catchments within the Valles Caldera National Preserve in north central New Mexico that feed into the East Fork of the Jemez River (Figure 1). The Valles Caldera (VC), which is part of the Jemez Mountains volcanic field (Orem and Pelletier, 2016), was the result of a series of eruptions that occurred between 1.61 and 1.12 Ma (Chipera et al., 2008; Wolff et al., 2011; Moravec et al., 2020). The intensive volcanic activity following the formation of the caldera made the underlying geology within the VC and its surroundings highly heterogeneous (Goff et al., 2011; Wolff et al., 2011).

Redondo Peak is the highest point in the VC at an elevation of approximately 3,435 masl. The Otowi and Tshirege members of the Bandelier Tuff comprise the majority of the geology of Redondo Peak (Nielson and Hulén, 1984). The Upper Jaramillo (3,055 km<sup>2</sup>,

La Jara (3,672 km<sup>2</sup>), and History Grove (2,421 km<sup>2</sup>) catchments that drain Redondo Peak (Figure 1), convey water toward the East Fork Jemez River, which is a tributary of the Rio Grande River (Lyon et al., 2008; Zapata-Rios et al., 2015, 2016). La Jara and History Grove watersheds have a predominant eastern aspect, whereas Upper Jaramillo catchment drains the northern side of the mountain (Zapata-Rios et al., 2016). Previous studies have argued that the predominant source of water in the Redondo Peak system is groundwater (Liu et al., 2008a; Lyon et al., 2008; Zapata-Rios et al., 2015; McIntosh et al., 2017; Olshansky et al., 2018b; White et al., 2019).

The climate at the VC has been classified as sub-humid-to-semi-arid due to its location between the snow-dominated Rocky Mountains and the monsoon-dominated southwestern United States (Zapata-Rios et al., 2016; McIntosh et al., 2017; White et al., 2019). The average precipitation recorded at the nearby Quemazon station is approximately 710 mm, of which approximately 40% falls as snow during winter and the remaining rainfall occurs during the summer monsoons (Broxton et al., 2009; Zapata-Rios et al., 2016; McIntosh et al., 2017). The average temperature at the VC is about 9 °C, ranging between 25 °C in the summer and −15 °C in the winter (Broxton et al., 2009; McIntosh et al., 2017). The forests at the VC elevations studied herein are dominated by spruce-fir and mixed conifer forests. Engelmann spruce (*Picea engelmannii*) and corkbark fir (*Abies lasiocarpa* var. *arizonica*) species are found in the highest elevations around the Redondo Peak (above 2,700 masl). Mixed conifer forest ranges between 2,500 and 3,100 masl, and grassland species are found around the dome between 2,500 and 3,200 masl (Zapata-Rios et al., 2016).

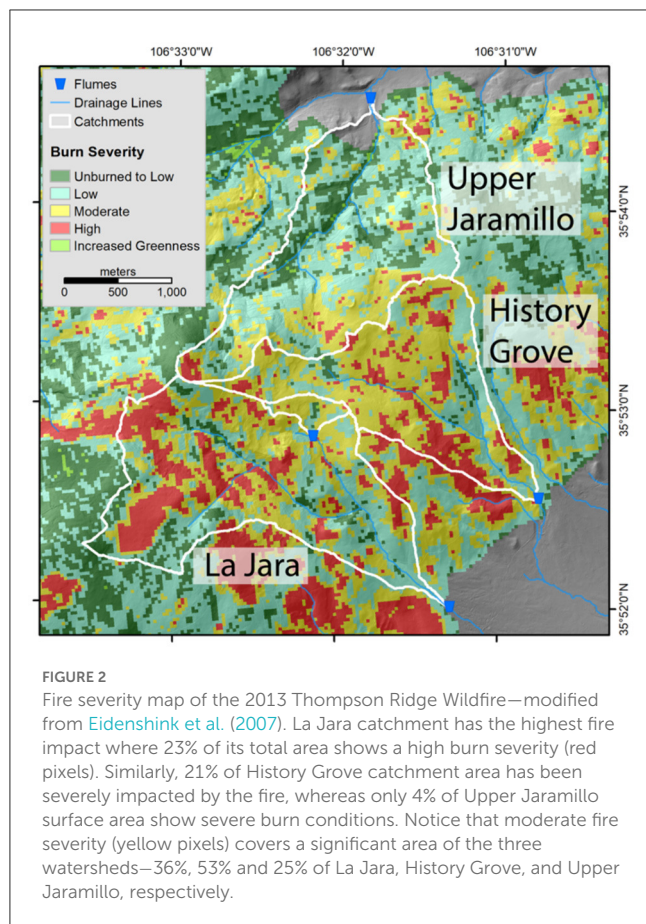


FIGURE 2

Fire severity map of the 2013 Thompson Ridge Wildfire—modified from Eidenshink et al. (2007). La Jara catchment has the highest fire impact where 23% of its total area shows a high burn severity (red pixels). Similarly, 21% of History Grove catchment area has been severely impacted by the fire, whereas only 4% of Upper Jaramillo surface area show severe burn conditions. Notice that moderate fire severity (yellow pixels) covers a significant area of the three watersheds—36%, 53% and 25% of La Jara, History Grove, and Upper Jaramillo, respectively.

The climatic conditions and the landscape of the VCNP make it susceptible to wildfires. Evidence from tree ring data suggests that dry atmospheric conditions preceded by years of wet conditions have a strong association with forest fires at the VC. The Thompson Ridge Wildfire burned from 31 May to 1 July 2013 and covered an area of ~23,965 acres (Cerrato et al., 2016). Moderate to high burn severities occurred in much of the three headwater catchments of the JRB-CZO (Figure 2). Post-fire debris flows that occurred following the first monsoon storms destroyed the gauging stations installed at the outlet of the La Jara and History Grove catchments creating a gap of ~3 years of missing discharge data that was filled using continuous monitoring from an adjacent catchment. Pre- and post-fire data were used in this study to investigate the impacts of wildfire in catchment hydrobiogeochemistry.

## 2.2. Water sampling and analysis

Pre- and post-fire surface water samples were collected monthly from the outlet of each catchment during dry periods (i.e., pre-snowmelt and summer), and weekly to biweekly during snowmelt and summer monsoon wet seasons. Pre-fire samples comprise those collected during water years (WYs) 2011, 2012, and through May of 2013, while post-fire sampling corresponds to monsoon (beginning in July) 2013, as well as WYs 2014, 2015, 2016, 2017, 2018, and 2019. Additionally, pre- and post-fire surface water

samples were collected from the nested zero order basin (ZOB) located at the top of La Jara catchment (Figure 1).

Temperature, pH, dissolved oxygen, and electrical conductivity were measured in the field with an Accumet AP84 (Fisher Scientific) multiprobe. Surface water samples for analysis of major cations, Si and Al were collected in acid-washed HDPE bottles. Samples for DIC, DOC, and anions chemistry were collected in combusted amber glass bottles. All the water samples were properly packed, stored at 4°C, and transported to The University of Arizona laboratory facilities for subsequent analysis.

Prior to water chemistry quantification, prewashed 0.45 μm nylon membranes were used to filter the aqueous aliquots for cation and Si analyses. Samples for DIC and DOC were filtered using combusted 0.7 μm glass-fiber filters. Chemical analyses were conducted in the Arizona Laboratory for Emerging Contaminants (ALEC) at the UA. Major cations (Na<sup>+</sup>, K<sup>+</sup>, Ca<sup>2+</sup>, and Mg<sup>2+</sup>), Si, Al, and Fe were analyzed by ICP-MS. Dissolved organic and inorganic carbon, and total dissolved nitrogen were analyzed on a Shimadzu TOC-VCSH Carbon analyzer (Shimadzu Scientific Instruments, Columbia, MD). Major anions (Cl<sup>-</sup>, NO<sub>3</sub><sup>-</sup>, and SO<sub>4</sub><sup>2-</sup>) were measured using ion chromatography (Dionex ICS-1000). Organic carbon characterization was measured via UV-Vis absorbance (Shimadzu Scientific Instruments UV-2501PC) and fluorescence excitation-emission matrices (EMMs) (Fluorescence spectrometer FluoroMax-4) (Perdrial et al., 2014; Vázquez-Ortega et al., 2015; Trostle et al., 2016). These spectroscopic characterizations of the dissolved organic matter (DOM) were used to calculate useful indices of DOM molecular structure including specific UV absorbance (SUVA), fluorescence index (FI), and humification index (HIX). Full multi-year datasets of surface water chemistry for Upper Jaramillo, La Jara and History Grove catchments are made available through HydroShare (McIntosh et al., 2021).

## 2.3. Flux calculations and impacts of fire severity

Annual fluxes for Na<sup>+</sup>, K<sup>+</sup>, Ca<sup>2+</sup>, Mg<sup>2+</sup>, Si, Al, Fe, Cl<sup>-</sup>, NO<sub>3</sub><sup>-</sup>, SO<sub>4</sub><sup>2-</sup>, DIC, DOC, and TDN were estimated using the mean flow method (Godsey et al., 2009; McIntosh et al., 2017). Volume-weighted mean concentrations (VWM) [mmol L<sup>-1</sup>] for each water year were calculated using Equation (1):

$$VWM = \frac{\sum_{i=1}^n C_i Q_i}{\sum_{i=1}^n Q_i} \quad (1)$$

where subscript *i* indicates each sampling day during the water year; *Q<sub>i</sub>* and *C<sub>i</sub>* are the daily average discharge [m<sup>3</sup>s<sup>-1</sup>] and solute concentrations [mmol L<sup>-1</sup>], respectively, of the *i<sub>th</sub>* day when the sample was collected. The annual water yield (AWY) [m y<sup>-1</sup>] of each catchment was then estimated using Equation (2):

$$AWY = \frac{\sum_{i=1}^n Q_i}{A} \quad (2)$$

where *Q<sub>j</sub>* is the daily streamflow record, and *A* is the estimated catchment area [m<sup>2</sup>]. Finally, annual flux of each solute (SF) [mmol

$m^{-2} y^{-1}]$  was estimated by multiplying *VWM* and *AWY*

$$SF = VWM \cdot AWY \quad (3)$$

## 2.4. Flow reconstruction

The calculations presented above are sensitive to daily discharge data. Streamflow measurements were interrupted during the WYs 2014, 2015, 2016, and part of 2017 in La Jara and History Grove catchments due to the post-fire debris flow during the monsoon season of WY 2013 that damaged the gauging flumes installed at each location. This missing information represents a challenge to solute flux calculations and the overall purposes of this study. Nevertheless, in spring of WY 2017 these flumes were replaced, thereby resuming post-fire streamflow records. Moreover, Upper Jaramillo flow observations were not discontinued throughout the pre- and post-fire WYs. We took advantage of these readily available data and other climate variables to estimate and reconstruct flows of La Jara and History Grove Creeks during the post-fire WYs of missing data.

Gaps in records, often unrecoverable, affect data analysis and interpretation (Harvey et al., 2012). Advances in hydrological modeling, however, have targeted and improved data infilling techniques to overcome this issue (Zhang and Post, 2018). A current focus in hydrology is to use numerical models, such as artificial neural networks (ANN), to infill missing daily streamflow (Ilunga and Stephenson, 2005; Kişi Özgür, 2007; Kim and Pachepsky, 2010; Wu and Chau, 2010; Shiau and Hsu, 2016; Petty and Dhingra, 2018). ANNs mimic the human neural system by acquiring knowledge through input and output variables. We built an ANN model to reconstruct the missing flow observations of La Jara and History Grove catchments, hereinafter referred as “target catchments.” The input independent variables utilized in the model were discharge from the neighboring catchment (Upper Jaramillo), total precipitation, snow water equivalent (SWE), and temperature obtained from the SNOTEL Quemazon station. We utilized only post-fire data to run the model since streamflow regimes may significantly differ from pre-fire conditions.

We utilized observed post-fire streamflow data from the target catchments, along with the other input variables, to train, validate, and test the model. The Levenberg-Marquardt algorithm was used to run the model. This algorithm minimizes the root square error between real observations and simulations of the streamflow data (Moré, 1978; Kim and Pachepsky, 2010). It has been shown that this algorithm produces fast and reliable results when training moderate-sized feedforward neural networks (Demuth et al., 1994). Normalized data were used to run the simulations. Program codes, including Neural Network Toolbox, were written, and run in MATLAB (The Math Works, Inc. *MATLAB*. Version 2020a). An ANN model was developed for each target catchment using the same input variables.

In each simulation we selected the optimal number of hidden neurons that had the least validation mean square error (MSE). Then training, validation, and testing simulations were performed, and regression scatter plots of streamflow (i.e., observed vs. simulated diagrams) were generated for each simulation step to

assess the model performance. Finally, the model with the best fit was utilized to infill the streamflow gap in each target catchment.

## 2.5. Burn severity estimates

The burn severity map of the Thompson Ridge Fire was obtained from the Monitoring Trends in Burn Severity program (MTBS). This program generates fire maps and data across the United States and classifies burn severity into high, moderate, and low (Eidenshink et al., 2007). We used the geospatial map of the Thompson Ridge Wildfire generated by MTBS to delineate the three watersheds studied herein (Figure 2). Moreover, we estimated the percentage of each burn severity class for each watershed using a pixel-based area estimation approach (Supplementary Table S5). Computations were made using ArcGIS 10.7.1 software.

## 2.6. Fire intensity impact on solute fluxes and water yields

In order to assess whether there is relationship between fire severity and the magnitude of solute exports across the three catchment we compared solute VWMs relative to their pre-fire average values using the following unitless metric:

$$\Delta X_{i,t} = \frac{X_{i,t}}{\bar{X}_{pre-fire_i}} \quad (4)$$

where *X* represents the VWM of each solute *i* at a given water year *t*.  $\bar{X}_{pre-fire_i}$  is the solutes average pre-fire VWM. Moreover, we also computed the relative change of AWY in each catchment using Equation (4). Nonetheless, AWY values were corrected to maximum SWE of each year to counter the effect of water input on runoff generation in each catchment.

## 3. Results

### 3.1. Post-fire climate, streamflow, and burn severity estimates

The calculated percentages of each burn severity class showed that 23% of La Jara catchment was severely burned. History Grove catchment burned in similar intensity—21% of its total surface area reported to have a high burn severity (Figure 2). Conversely, only 4% of Upper Jaramillo catchment seemed to have high burn intensity levels. Moreover, while over 90% of La Jara and History Grove catchments had been impacted by the fire, 75% of Upper Jaramillo burned, being the upper part of the catchment where most of the fire impacts occurred (Figure 2).

Pre- and post-fire average air temperature ranged from 25°C in the summer to −12°C in the winter. Intense rainfall events occurred during the summer monsoons (July through September), with WY 2013—the monsoon season immediately after the wildfire—the wettest and WY 2017 the driest accumulating approximately 400 mm and 21 mm of total rainfall respectively (Figure 3A). Similarly, winter precipitation varied significantly

across the pre- and post-fire WYs. Pre-fire deep snowpacks were reached in WY 2012 (191 mm of maximum SWE), whereas the post-fire WY 2019 reported the largest snow accumulation (264 mm of maximum SWE). Conversely, the driest pre- and post-fire winters corresponded to WYs 2011 and 2018 with SWE peaking at 96 mm and 35 mm, respectively (Figure 3B).

The ANN training, validation and testing results are summarized in the supplementary material (Supplementary Figure S1). After the visual inspection and comparison of the error statistics, the ANN model of La Jara Creek seems to well predict post-fire discharge—regression coefficients are above 0.95 ( $p < 0.05$ ) for validation and testing (Supplementary Figure S1A). Although some over- and under-predictions are observed in History Grove post-fire runoffs, validation and testing regression coefficients are still significant (above 0.80,  $p < 0.05$ , Supplementary Figure S1B). Moreover, the infilled post-fire discharges of La Jara and History Grove Creeks agreed with the observed increments of Upper Jaramillo stream flows relative to pre-fire surface water discharges (Figure 3C).

The overall post-fire stream discharges were consistently higher than pre-fire surface water flows in La Jara, History Grove, and Upper Jaramillo catchments (Figure 3C). It is noteworthy that peak discharge values in 2015 were higher than in 2016 and 2017 despite lower SWE. Nevertheless, the consistent dry conditions that prevailed from summer 2017 until winter/spring 2018 resulted in significantly reduced streamflow in the three creeks during WY 2018 (Figure 3C). Peak flows were typically reached in late March to early April (spring snowmelt), with post-burn streamflow rates  $\sim 10$  times higher than pre-burn peak flows (Figure 3C). Moreover, greater, and more persistent stream discharges are observed during the post-fire summer monsoons (July through September) than pre-fire stream flows.

## 3.2. Base cation concentrations

Immediate post-burn pulses of major cations— $\text{Na}^+$ ,  $\text{K}^+$ ,  $\text{Ca}^{2+}$ , and  $\text{Mg}^{2+}$ —were observed in the three watersheds and remained elevated for the majority of the monsoon season in 2013 (Figure 4). Moreover, post-fire concentrations (i.e., during WY 2014 through WY 2019 that followed the monsoon of 2013) were lower than the initial pulses, despite remaining higher than pre-burn levels (Figure 4). Volume-weighted means (VWM) of bivalent cations, i.e.,  $\text{Ca}^{2+}$  and  $\text{Mg}^{2+}$ , were the highest immediately after burning (summer of WY 2013) in the three catchments and were consistently high throughout the post-fire period relative to pre-burn background concentrations (Supplementary Figure S2, Table S3).

Post-fire responses of monovalent cations ( $\text{Na}^+$  and  $\text{K}^+$ ) were significantly higher compared to pre-fire levels. Sodium and  $\text{K}^+$  VWMs increased in the initial months after burning (end of WY 2013), and during WYs 2014 and 2015. Nonetheless, in the later years after the fire (WYs 2016, 2017, 2018, and 2019),  $\text{Na}^+$  and  $\text{K}^+$  concentrations decreased, mirroring pre-fire baselines (Supplementary Figure S2, Table S3). Conversely, VWM concentrations for Si showed no significant differences before and after burning among the three watersheds, i.e., no immediate pulse

or changes in surface water concentrations are observed during the post-fire WYs (Supplementary Figure S2, Table S3).

All major cations and Si were subjected to higher fluxes after burning relative to pre-fire baselines, except in WY 2018 when the relative dry conditions and reduced surface water flows decreased solute mobilization (Figure 5). This increase in flux is due to the combined effects of VWM concentration change and increased discharge. Overall, base cations and Si exports were the highest in La Jara Creek with the early post-fire years (WYs 2014, 2015, and 2016) reporting the highest fluxes (Figure 5). Effluxes of these solutes in History Grove and Upper Jaramillo Creeks also peaked in the early post-fire period (WY 2015)—although in less magnitude than La Jara Creek. Slightly higher exports of major cation and Si were, nevertheless, observed in History Grove than Upper Jaramillo surface waters (Figure 5). These solute rate differences may be linked to fire severity and hydrologic regimes of each catchment.

## 3.3. Polyvalent cations

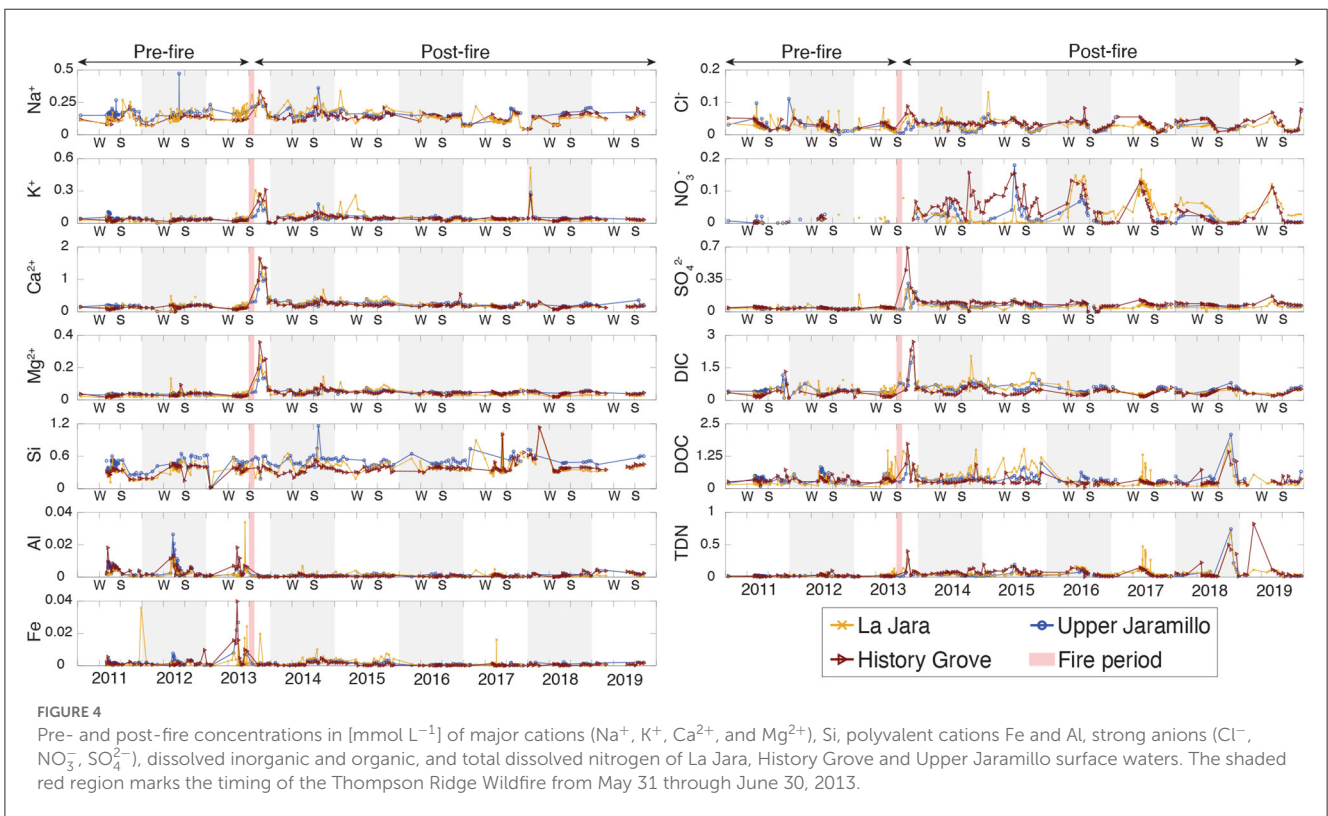
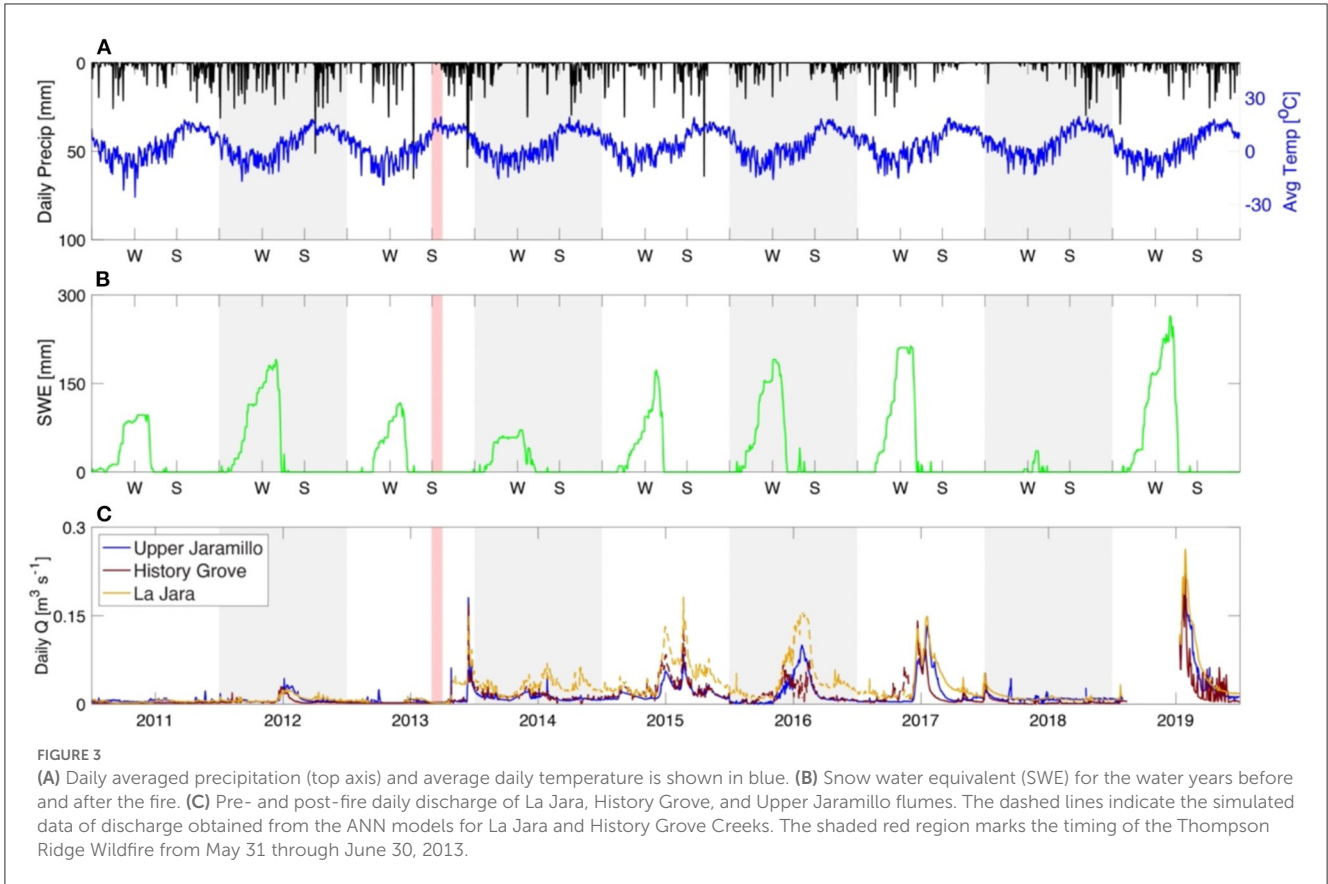
The responses of polyvalent hydrolyzing cations (Al and Fe) differ from non-hydrolyzing base cations and Si as they showed reduced concentrations post-fire. Peak exports of these elements were observed during pre-burn snowmelt periods. Post-fire Al and Fe concentrations, however, did not show such a pattern (Figure 4). Iron and Al VWMs were consistently lower in the post-burn period in the surface water of History Grove and Upper Jaramillo Creeks relative to pre-burn conditions (Supplementary Figure S2, Table S3). High Fe concentrations, however, were observed in La Jara catchment during the post-burn WYs 2014 and 2015. These concentrations decreased below pre-fire levels in the subsequent post-fire years (WYs 2016 through 2019). Moreover, La Jara Creek Al concentrations were consistently lower in the post-fire period compared to pre-fire underlying concentrations (Figure 4, Supplementary Figure S2, Table S3).

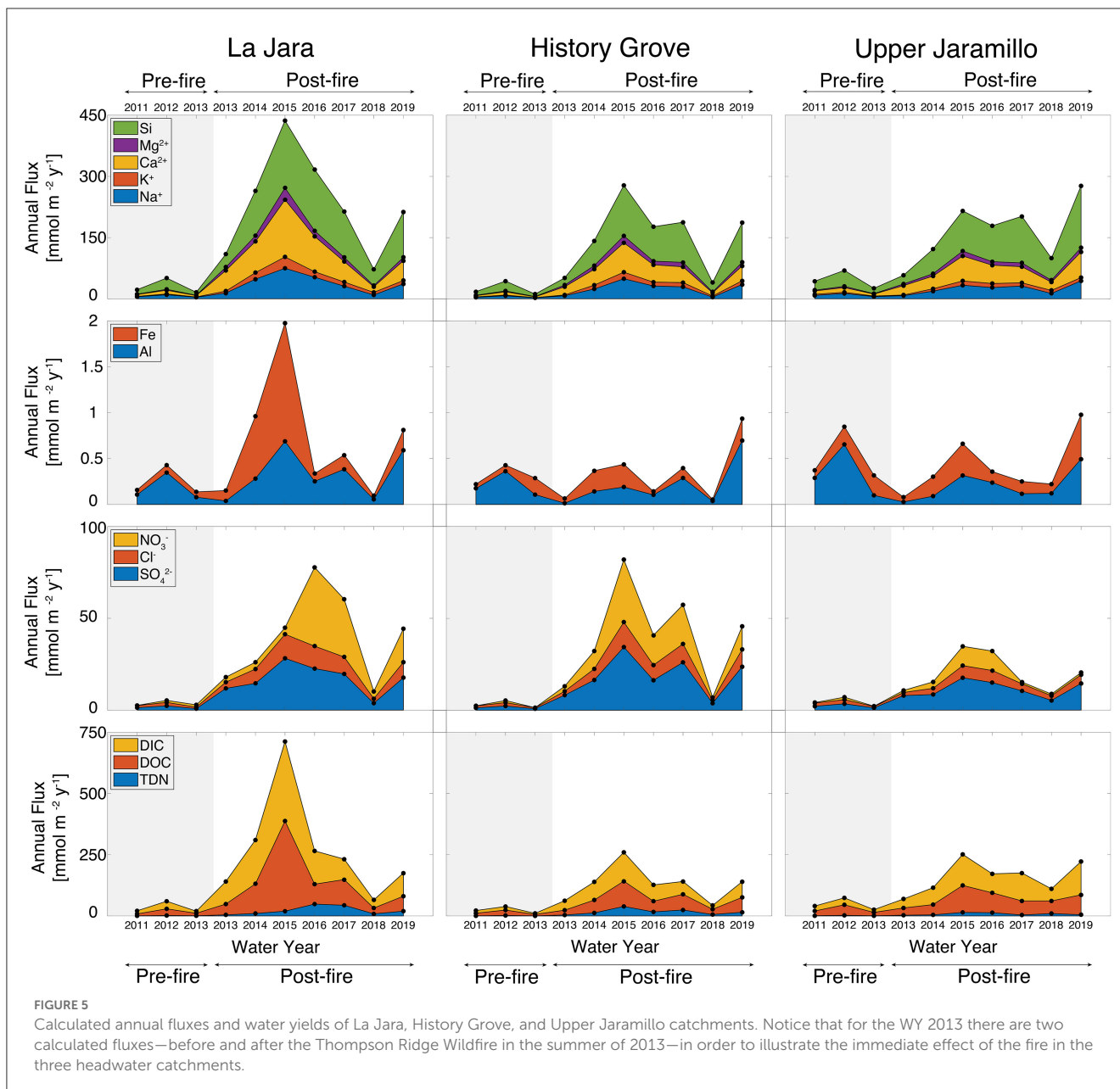
The highest Fe and Al fluxes in La Jara Creek were observed in WY 2015 (1.29 and 0.69  $\text{mmol m}^{-2} \text{y}^{-1}$ , respectively, Figure 5). History Grove and Upper Jaramillo Creeks showed significant Fe outflows in WY 2019 (0.25  $\text{mmol m}^{-2} \text{y}^{-1}$  and 0.48  $\text{mmol m}^{-2} \text{y}^{-1}$ , respectively, Figure 5). Moreover, History Grove also had the highest Al fluxes in WY 2019 (0.36  $\text{mmol m}^{-2} \text{y}^{-1}$ ), whereas Upper Jaramillo Al fluxes peaked during the pre-fire WY 2012 (0.66  $\text{mmol m}^{-2} \text{y}^{-1}$ , Figure 5).

## 3.4. Anions

Large pulses of  $\text{NO}_3^-$  in stream water are observed in the six-year post-fire period in La Jara, History Grove, and Upper Jaramillo catchments. The second, third, and fourth year after burning (WYs 2015, 2016, and 2017) showed the highest peak concentrations of  $\text{NO}_3^-$  during periods of high discharge, i.e., spring snowmelt, in the three creeks. In contrast, during winter base flow periods,  $\text{NO}_3^-$  exports decreased significantly, reaching values close to pre-fire observations (Figure 4).

Nitrate VWMs in the surface waters of the three watersheds were higher than pre-fire baselines at the beginning of the





post-fire period (end of WY 2013 and WY 2014). The highest VWMs were observed during WYs 2015, 2016 and 2017 reaching concentrations above  $0.06 \text{ mmol L}^{-1}$  in Upper Jaramillo Creek, and  $0.1 \text{ mmol L}^{-1}$  in La Jara and History Grove surface waters (Supplementary Figure S2, Table S4). Similarly, the highest  $\text{NO}_3^-$  fluxes were observed during WYs 2015 and 2016— $\text{NO}_3^-$  annual fluxes surpassed  $34 \text{ mmol m}^{-2} \text{ y}^{-1}$  in La Jara and History Grove catchments, and exports above  $10 \text{ mmol m}^{-2} \text{ y}^{-1}$  were observed in Upper Jaramillo (Figure 5). It is important to point out that  $\text{NO}_3^-$  VWMs and fluxes decrease toward the end of the post-fire period (WYs 2017 through 2019) in the three catchments (Figure 5, Supplementary Figure S2).

Sulfate concentrations in the streams reached a maximum of  $0.35$  to  $0.7 \text{ mmol L}^{-1}$  at the beginning of the post-fire period (monsoon season of WY 2013, Figure 4). Furthermore, during

the six-year period after burning (WY 2014 through WY 2019),  $\text{SO}_4^{2-}$  concentrations in La Jara, History Grove and Upper Jaramillo Creeks remained below  $0.2 \text{ mmol L}^{-1}$  and showed little variability (Figure 4). However, the mean  $\text{SO}_4^{2-}$  concentrations in the three burned catchments were consistently higher than pre-fire baselines. These patterns mirror that of the lithogenic element post-fire fluxes— $\text{K}^+$ ,  $\text{Ca}^{2+}$ , and  $\text{Mg}^{2+}$ .

Sulfate VWMs and fluxes were consistently higher during the six-year period after the wildfire than the pre-fire  $\text{SO}_4^{2-}$  fluxes in La Jara, History Grove, and Upper Jaramillo Creeks (Figure 5, Supplementary Figure S2, Table S3). The highest fluxes occurred in WY 2015 reaching  $28.23$ ,  $34.37$ , and  $17.61 \text{ mmol m}^{-2} \text{ y}^{-1}$  in La Jara, History Grove, and Upper Jaramillo respectively. These outflows were consistently high throughout the post-fire period, except in WY 2018, when low precipitation and surface water

discharges decreased these exports relatively close to pre-fire levels (Figure 5).

Chloride concentrations were elevated immediately after the fire (Figure 4); this initial pulse, however, was smaller than that of  $\text{SO}_4^{2-}$ . Even though  $\text{Cl}^-$  concentrations showed similar variability in both pre- and post-fire WYs, there was an overall increase of  $\text{Cl}^-$  concentrations after burning in La Jara, History Grove, and Upper Jaramillo Creeks (Figure 4)—although they were smaller relative to  $\text{NO}_3^-$  and  $\text{SO}_4^{2-}$  concentrations increases.

Chloride highest VWMs were observed immediately after burning (end of WY 2013) in the three catchments. History Grove  $\text{Cl}^-$  VWMs were slightly higher than pre-fire levels throughout the post-fire period (WYs 2014 through 2019), ranging from 0.034 to 0.42  $\text{mmol L}^{-1}$ . Conversely, La Jara and Upper Jaramillo  $\text{Cl}^-$  VWMs were at or below pre-fire background concentrations, especially during the late post-fire period (WYs 2017 through 2019, Supplementary Figure S2, Table S4). Chloride peak fluxes were reached in the early post-fire period (WY 2015) in the three catchments, and thereafter declined consistently toward the end of the post-fire period (Figure 5).

### 3.5. Dissolved inorganic and organic carbon and total dissolved nitrogen

La Jara, History Grove and Upper Jaramillo Creeks showed a large pulse of dissolved inorganic and organic carbon, and total dissolved nitrogen immediately after the fire (monsoon season of WY 2013), reaching values of 2.7, 1.7 and 0.4  $\text{mmol L}^{-1}$  of DIC, DOC and TDN respectively (Figure 4). These observations are consistent with the initial responses of base cations and anions described above. Furthermore, DIC concentrations were elevated in WYs 2014 and 2015 relative to pre-fire values, whereas from WY 2016 to WY 2019 DIC decreased and were closer to pre-burn baselines. During the late post-fire period, however, these concentrations showed much less variability than during the early years after burning (Figure 4).

Dissolved organic carbon showed more variability during the post-fire WYs than during the pre-fire conditions. High DOC effluxes were observed in WYs 2014 and 2015 relative to the late post-fire WYs (Figure 4). Similarly, post-fire TDN concentrations increased after the fire and were consistently high during the six-year post-burn. Moreover, TDN and  $\text{NO}_3^-$  follow similar trends after burning, i.e., high discharges of these solutes correspond to the high surface flow periods (snowmelt season), whereas low concentrations occurred during baseflow conditions (Figure 4).

Dissolved inorganic and organic carbon VWMs, increased immediately after the wildfire (monsoon season 2013) and kept these high concentrations through WY 2015. Nonetheless, from WY 2016 to WY 2019, DIC and DOC VWMs decreased close to pre-burn concentrations. Total dissolved nitrogen VWMs remained above pre-fire levels during the six-year post-fire period (Supplementary Figure S2, Table S4).

Finally, DIC and DOC fluxes were the highest in WY 2015 in La Jara (325 and 368  $\text{mmol m}^{-2} \text{y}^{-1}$  of DIC and DOC, respectively) and History Grove (118  $\text{mmol m}^{-2} \text{y}^{-1}$  of DIC and 103  $\text{mmol m}^{-2} \text{y}^{-1}$  of DOC) catchments. These exports decreased toward the

end of the post-fire period (Figure 5). Conversely, Upper Jaramillo DIC fluxes peaked in WY 2019—over 135  $\text{mmol m}^{-2} \text{y}^{-1}$  of DIC—whereas 110  $\text{mmol m}^{-2} \text{y}^{-1}$  of DOC were flushed out of Upper Jaramillo catchment during WY 2015 (Figure 5). Total dissolved nitrogen showed increased fluxes and concentrations in La Jara, History Grove, and Upper Jaramillo Creeks compared to pre-fire baselines (Figure 5).

### 3.6. Burn intensity impacts and recovery

The relationships calculated using Equation (4) showed some variability between pre- and post-fire solute VWMs and AWYs in the three catchments (Figure 6). VWM concentrations of  $\text{Na}^+$ , Si,  $\text{Cl}^-$ , and DOC did not show significant differences relative to pre-fire values in La Jara, History Grove, and Upper Jaramillo streams. Conversely,  $\text{Ca}^{2+}$ ,  $\text{Mg}^{2+}$ ,  $\text{K}^+$ , DIC, and  $\text{SO}_4^{2-}$  exhibited significant increments, particularly immediately after the fire (end of WY 2013) and during WYs 2014 and 2015 (Figure 6). Moreover, the greatest increases in these solutes were observed for the severely burned La Jara and History Grove catchments. Smaller changes occurred in the moderately burned Upper Jaramillo catchment, but even these ratios remained higher than pre-fire baselines (Figure 6). Additionally, toward the end of the post-fire period (WY 2016 through WY 2019) these relative changes decreased, and it should be noted that the three surface waters presented similar magnitudes of these solute increments. This progressive decrease throughout the post-fire period might be indicative of system recovery.

Post-fire  $\text{NO}_3^-$  and TDN also showed significant increments relative to pre-fire backgrounds in the surface waters of La Jara, History Grove, and Upper Jaramillo, although peak discharges were delayed—maximum changes occurred between WY 2015 and WY 2017. We did not observe a clear relationship between burn severity and  $\text{NO}_3^-$  and TDN increments; the highest  $\text{NO}_3^-$  and TDN relative changes were, nonetheless, observed in History Grove Creek (Figure 6). Finally, post-fire Al and Fe decreased relative to pre-fire means, and similar values were observed in the three catchments. Nevertheless, in WYs 2014 and 2015 only La Jara Creek showed high Fe effluxes relative to pre-fire values (Figure 6), and related work indicates that these effluxes were largely in nanoparticulate form (Olshansky et al., 2018a).

Parallel to what was observed for daily discharge (Figure 3C), post-fire AWYs exhibited significant changes in La Jara, History Grove, and Upper Jaramillo Creeks relative to pre-fire water yields. Again, the highest increases occurred in the two catchments that were severely impacted by the wildfire (i.e., La Jara and History Grove), whereas Upper Jaramillo post-fire yields changed in less magnitude, although higher than pre-burn baseline (Figure 6). Moreover, it appears that these yields exhibited a steady decrease toward the end of the post-fire period presented in this study. It is important to point out that during the dry WY 2018, the AWYs showed experienced a relative increase.

## 4. Discussion

Comparisons of solute concentrations and fluxes in the short and long-term after a wildfire shed light on

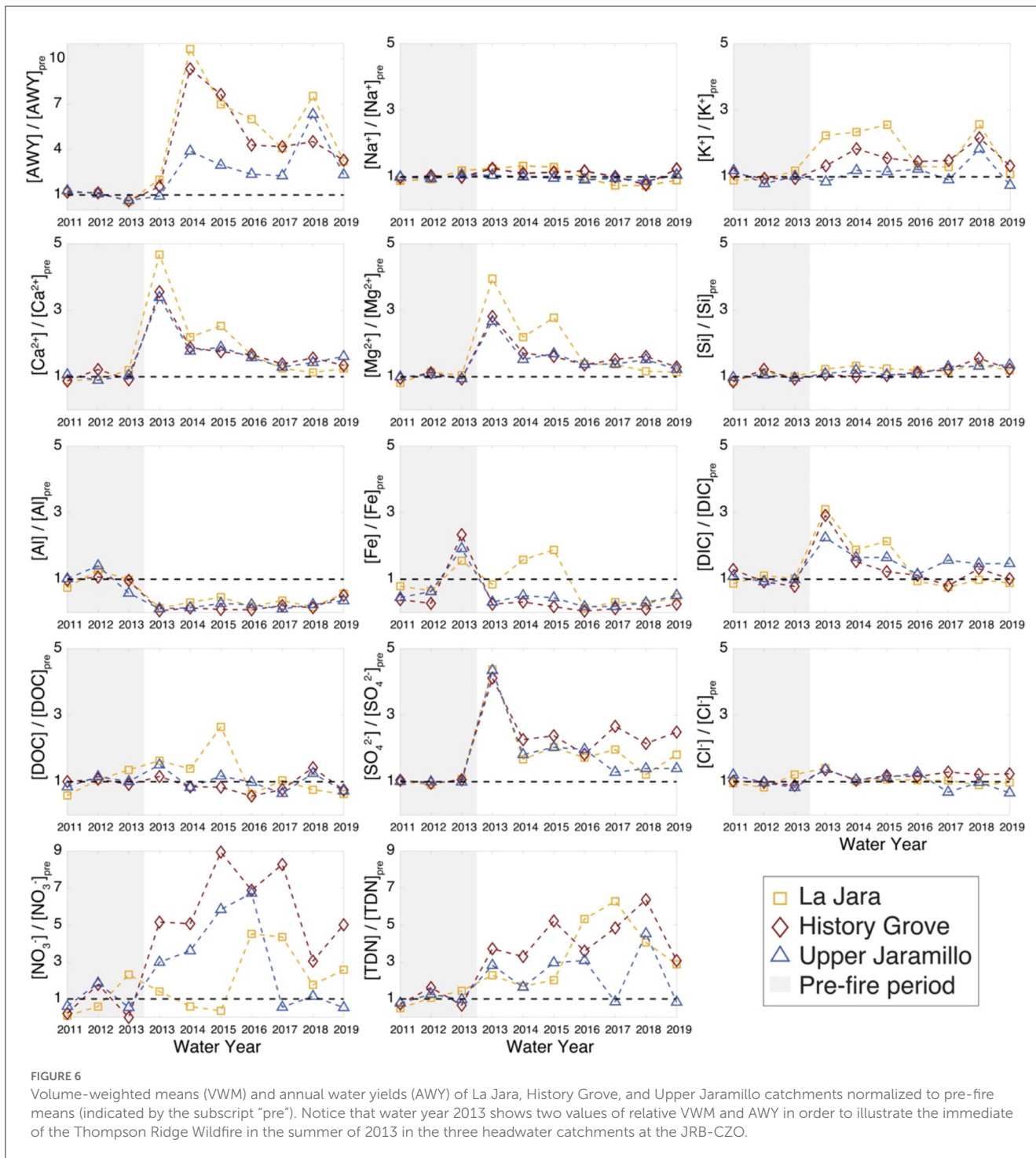


FIGURE 6  
Volume-weighted means (VWM) and annual water yields (AWY) of La Jara, History Grove, and Upper Jaramillo catchments normalized to pre-fire means (indicated by the subscript "pre"). Notice that water year 2013 shows two values of relative VWM and AWY in order to illustrate the immediate of the Thompson Ridge Wildfire in the summer of 2013 in the three headwater catchments at the JRB-CZO.

the evolution of the mineral-derived mass loss (chemical denudation) in fire-disturbed forested catchments and provide insights into how hydrologic and biogeochemical processes respond to these disturbances. Moreover, fire intensity seems to play a significant role on nutrient exports and water discharges across the three headwater catchments at the JRB-CZO.

### 4.1. Impact of fire intensity on solute and water effluxes

Fire frequency and burn severity may impact the magnitude of solute fluxes relative to pre-fire levels (Bayley et al., 1992a). For instance, our data showed that the highest increments of lithogenic element exports correspond to the severely burned La Jara

catchment followed by History Grove catchment (23% and 21% high burn severity, respectively). Conversely, Upper Jaramillo (4% high burn severity) showed the lowest shifts of these cation exports, and yet higher than pre-fire baselines (Figure 6). Furthermore, despite the relatively low proportion of Upper Jaramillo catchment area categorized as high burn severity, about 25% of its surface area has a moderate burn severity, which is consistent with its elevated nutrient ion losses above background levels for the six-year post-fire period presented in this study. This highlights the role of moderate to high burn areas on the long-term surface waters solute concentrations and fluxes in disturbed forested catchments. Nevertheless, toward the end of the post-fire period (WYs 2017, 2018, and 2019), similar solute losses were observed in the three catchments relative to their corresponding pre-fire levels (Figure 6). These observations reflect system resilience and capacity to regulate rates of solute and water loss after fire disturbance. Studies on surface water chemistry and watershed balances in mixed-conifer forests in the Sierra Nevada, California, have reported persistent high levels of base cations, nutrient anions, and water from 5 to 9 years after prescribed fires (Williams and Melack, 1997b; Engle et al., 2008). Thus, we expect that these fire-enhanced solute and water exports to remain higher than pre-fire baselines beyond the six-year post-fire period presented herein.

Moreover, catchment hydrology also plays a role on solute and water exports observed in the three headwater catchments at the JRB-CZO. Studies that have investigated aspect control on the hydro-biogeochemistry of the headwaters surrounding Redondo Peak found that predominantly north facing catchments, such as Upper Jaramillo, are characterized by deeper regolith, longer water residence times, more water availability, and larger concentrations of dissolved organic and inorganic materials (Perdrial et al., 2014; Zapata-Rios et al., 2015, 2016). These water regimes may prolong solute mobilization in the surface waters of Upper Jaramillo Creek after the fire despite its relatively low burn severity. Conversely, the higher hydraulic connection between the streams and groundwater, and larger energy inputs in east-facing catchments (La Jara and History Grove) (Zapata-Rios et al., 2016; White et al., 2019) may quickly mobilize solutes through the surface and subsurface after the fire. Furthermore, increased post-fire SWE and surface water storages (Harbold et al., 2014; Maina and Siirila-Woodburn, 2020) allow water to flush quicker through the surface and near subsurface—particularly in La Jara and History Grove where stream discharges and water yields are significantly higher than pre-burn baselines (Figure 3C). These flashier responses and the much higher peak discharge values observed for 2015 than in 2016 and 2017 (despite lower SWE values for 2015) may have exhausted the pool of fire-derived solutes, thereby accounting for the progressive decrease in fluxes and VWM concentrations in the late post-fire period (Figures 5, 6).

The rapid and persistent response observed in the stream flow chemistry of the three headwater catchments following the wildfire likely respond to the system underlying lithology and hydrologic regimes. High solute concentrations in streams with sedimentary and granitic mixtures (Rhoades et al., 2011), and carbonate-bearing rock (Mast and Clow, 2008) mask post-fire changes in stream chemistry. Conversely, in naturally dilute systems, surface water chemistry may have a sharp response to disturbances such as fire (Rhoades et al., 2011). The rhyolitic volcanic rocks that dominate

the geology of the headwaters of the JRB-CZO rely on snowmelt to recharge the groundwaters and generate streamflow (Liu et al., 2008a; Zapata-Rios et al., 2015, 2016; McIntosh et al., 2017; White et al., 2019) generating relatively dilute surface waters (Olshansky et al., 2018b; White et al., 2019). Thus, post-fire catchment processes drive the initial and the long-lasting effect on surface water chemistry.

## 4.2. Post-fire biogeochemical drivers of solute exports

Estimated solute fluxes and relative changes of VWM concentrations showcase a progressive evolution of post-fire nutrient effluxes. An initial post-fire pulse of solutes—base cations,  $\text{SO}_4^{2-}$ ,  $\text{Cl}^-$ , DIC (and associated alkalinity as  $\text{HCO}_3^-$ ), DOC, and TDN is followed by a significant reduction of solute exports in the first- and second-year following fire. These concentrations, nevertheless, remained elevated above pre-fire levels. In the late post-fire period—years three to six after the fire—despite solute concentration decreases in the streams relative to the early post-fire years—most of these exports are still higher than pre-fire conditions. In this section we highlight the geochemical and biological catchment processes—sediment transport, weathering of fresh mineral surfaces, microbially-mediated reactions, and delayed biotic uptake—that drive the continuous chemical denudation in the short- and long-term of the forest biomantle after fire.

Ash deposits on hillslopes may be responsible for the initial sharp increase in surface water solute concentration. Depending on fire severity, low solubility aromatic pyrogenic carbon structures prevail in ash with high levels of initial organic carbon due to incomplete combustion. Conversely, highly soluble and mobile  $\text{Ca}^{2+}$ ,  $\text{Mg}^{2+}$ , and  $\text{K}^+$  carbonates and hydroxides are the main components of ash produced in hotly burned forests (Quill et al., 2010; Pereira et al., 2012, 2014; Bodí et al., 2014). Swindle et al. (2021) reported significant increments of base cations in stream water of a chaparral-dominated watershed after major precipitation events following a wildfire. The authors argued that leachates from ash were responsible for the initial high pulse of major cation concentrations in surface waters after fire. Chorover et al. (1994), Williams and Melack (1997b), and Murphy et al. (2006) also reported an immediate increase of base cations and anions (e.g.,  $\text{Cl}^-$ ,  $\text{SO}_4^{2-}$ , and  $\text{NO}_3^-$ ) concentrations in pore water and surface water solutions in burned mixed-conifer catchments of the Sierra Nevada, California. The strong agreement of our results with these investigations supports our contention that the initial pulse of solutes exported in the surface waters of La Jara, History, Grove, and Upper Jaramillo are due to leaching of water-extractable elements from ash deposits during the monsoon season that followed the wildfire in the summer of 2013 (Figure 4).

Studies in forested systems have shed light on the long-lasting effect of wildfires on pore-water and surface water geochemistry (Chorover et al., 1994; Williams and Melack, 1997b; Murphy et al., 2006; Engle et al., 2008; Rhoades et al., 2011, 2019; Näthe et al., 2018; Santos et al., 2019; Granath et al., 2021). Bivalent base cations (i.e.,  $\text{Ca}^{2+}$  and  $\text{Mg}^{2+}$ ) and strong acid anions (i.e.,  $\text{SO}_4^{2-}$ ,  $\text{NO}_3^-$  and  $\text{Cl}^-$ ) may exceed pre-fire concentrations for

up to 5 years post-fire (Williams and Melack, 1997b; Rhoades et al., 2011; Santos et al., 2019). Moreover, high magnitude erosion events, e.g., debris flows, account for the majority of the long-term landscape denudation and sediment export in burned watersheds (Smith et al., 2012; Orem and Pelletier, 2016), may redistribute and store fine sediments that contain ash in marginal levees and flow deposits along valleys and channel sections with low slopes (Reneau et al., 2007; Smith et al., 2012). As spring snowmelt and summer monsoon seasons reoccur, these deposits increase fine and dissolved sediments exports that may remain above pre-fire levels for at least 5 years after burning (Reneau et al., 2007). The debris flow that followed the Thompson Ridge Fire in 2013 may have redistributed ash-bearing sediments along streams and valley bottoms around Redondo Peak, increasing post-fire solute and sediment exports. Thus, increased exports of suspended and dissolved materials may be responsible for the high rate of solute effluxes during the six-years post-fire period relative to the background pre-fire levels in the three headwater catchments at the JRB-CZO. Additionally, rock spalling and vertical fracturing after burning enrich substantially rock fragment content in soils, i.e., soil stoniness (Shtober-Zisu and Wittenberg, 2021). As more water moves on soil surfaces and through the near subsurface due to increased overland flows after burning (Humphreys et al., 2003; Jung et al., 2009), these thermally damaged rocks are more susceptible to physical and chemical erosion (Goudie et al., 1992; Allison and Bristow, 1999; Humphreys et al., 2003; Shtober-Zisu et al., 2015; Buckman et al., 2021). Thus, in addition to the enhanced transport of suspended and dissolved materials after fire, these near surface weathering reactions may partly account for the elevated concentration of major cations (e.g.,  $\text{Ca}^{2+}$ ,  $\text{Mg}^{2+}$ , and  $\text{K}^+$ ) during the six-year period after the fire. Nevertheless, further research is encouraged to assess the direct effect of fires on weathering reactions.

Forest soils may undergo an increase in cation exchange capacity (CEC) due to burning. These changes may be due to increase of specific surface area (SSA) (Araya et al., 2016) and presence of black carbon (Liang et al., 2006) after burning. Chorover et al. (1994) observed that the concentration of  $\text{Ca}^{2+}$  and  $\text{Mg}^{2+}$  in soil solutions remained elevated 3 years after fire. The authors argued that these responses may be due to the higher affinity of ion exchange sites for these cations. Thus, ion selectivity and augmented CEC may drive transfer and transport rates of cations—particularly the bivalent cations—from burned soils to streams and may account for the elevated concentration of  $\text{Ca}^{2+}$  and  $\text{Mg}^{2+}$  during the six-year post-fire period compared to anticipated faster migration of their monovalent counterparts, particularly  $\text{Na}^+$ , which tends to exhibit relatively low selectivity for ion exchange sites, but also  $\text{K}^+$ .

Furthermore, prolonged increases in  $\text{SO}_4^{2-}$  likely enhance base cations exports after wildfires, particularly bivalent cations  $\text{Ca}^{2+}$  and  $\text{Mg}^{2+}$ . Increased surface water  $\text{SO}_4^{2-}$  concentrations after burning have been observed in other forested systems (Bayley et al., 1992b; Chorover et al., 1994; Williams and Melack, 1997b). Williams and Melack (1997b) found a significant correlation between  $\text{SO}_4^{2-}$  and the sum of  $\text{Ca}^{2+}$  and  $\text{Mg}^{2+}$  suggesting the central role of fire-induced oxidation of organic sulfur in the charge balanced catchment export of cations. Elevated post-fire

concentrations of  $\text{SO}_4^{2-}$  in the surface waters of the JRB-CZO evidently also mediate the loss of  $\text{Ca}^{2+}$  and  $\text{Mg}^{2+}$  during the post-fire period.

Forests regulate  $\text{SO}_4^{2-}$  and  $\text{Cl}^-$  exports by biotic uptake and retention in living and dead organic matter (Chorover et al., 1994; Williams and Melack, 1997b). Forest floor recovery may enhance biotic uptake and formation of S- and Cl-bearing organic molecules in soils, thereby retaining and decreasing mobilization of  $\text{SO}_4^{2-}$  and  $\text{Cl}^-$  after fire (Williams and Melack, 1997a; Vodyanitskii and Makarov, 2017; Santos et al., 2019). Furthermore,  $\text{Cl}^-$  in soils can accumulate in biomass, e.g., forming halogenated organics ( $\text{Cl}_{\text{org}}$ ) (Montelius et al., 2015; Svensson et al., 2021). Biomass depletion, due to forest fires, may decrease soil chlorination processes (Gustavsson et al., 2012), thus more  $\text{Cl}^-$  ions may be transferred to streams, particularly during the early post-fire period, as evident in  $\text{Cl}^-$  VWM concentrations and fluxes in the three burned watersheds (Figure 5, Supplementary Figure S2). Moreover, as the forest floor recovered from burning,  $\text{Cl}_{\text{org}}$  pools likely accumulated, thereby decreasing the amount of  $\text{Cl}^-$  exported, returning to pre-fire levels during the late post-fire WYs. Additionally, other nutrient ions may also respond to nutrient uptake resilience after fire. For instance,  $\text{K}^+$  is highly mobile in plant tissues and is an essential nutrient required for plant growth and maintenance (Williams and Melack, 1997b; Kramer, 2012). Thus, the significant decrease of  $\text{K}^+$  concentrations, compared to  $\text{Na}^+$ , 3 years after burning—particularly in La Jara Creek—suggests  $\text{K}^+$  bio-uptake due to biomass recovery after fire.

These patterns observed in  $\text{NO}_3^-$  and TDN post-fire concentrations in the streams may be a response to biological activity and N availability in soils. Combustion of organic matter mineralizes organic nitrogen to ammonium ( $\text{NH}_4^+$ ). Depending on fire severity, microbial biomass in the surface soil layers (0–5 cm) can be completely eradicated, and up to a 50% reduction of microbial communities can be reached even in deeper mineral soil (5–10 cm) (Gustine et al., 2022). Therefore, the relatively low  $\text{NO}_3^-$  concentrations, and the associated TDN, in the early post-fire period (end of WY 2013 and WY 2014) reported in this study may be the result of decreased nitrifier activity, resulting in the persistence of N in ammonium form. As soil microbial communities recover, high levels of both exchangeable  $\text{NH}_4^+$  and  $\text{NO}_3^-$  indicate high nitrification potentials in burned compared to undisturbed soils (Hernández et al., 1997). Thus, one expects a lag in nitrate loss, relative to loss of mobile elements accumulated in ash. This is indeed the case in the post-fire JRB-CZO, where  $\text{NO}_3^-$  leached from soils to streams resulted in a pulse 2–4 years postfire (Figures 4, 5, Supplementary Figure S2), lagging significantly behind the pulsed losses of base cations and sulfate. Moreover, it has been argued that inorganic N loads in surface waters of mixed-conifer catchments are likely influenced by runoff (Williams and Melack, 1997b). This agrees with the reduced  $\text{NO}_3^-$  fluxes observed in the three streams during the dry WY 2018. Furthermore, progressive vegetation and microbial uptake may be responsible for the gradual reduction of stream water  $\text{NO}_3^-$  concentrations toward the end of the post-fire period in the three watersheds (Figures 4, 5, Supplementary Figure S2) as forest floors nitrogen pools decrease (Gustine et al., 2022).

The significant decrease in concentration and flux of polyvalent cations, Al and Fe, after the fire could signal diminished complexation with soluble organic matter and therefore retention in the system. These weathering-derived solutes are transported by complexation with organic matter and/or as colloids during periods of soil saturation, e.g., spring snowmelt (Trostle et al., 2016; McIntosh et al., 2017; Olshansky et al., 2018a). It has been argued that the *ortho*-dihydroxy functional groups, present in phenolic monomers, likely favor complexation of soil organic matter with these polyvalent cations (Shindo and Kuwatsuka, 1977; Vance et al., 1986; Gallet and Pellissier, 1997), thereby increasing their solution phase concentration and mobilization from soil to surface waters when saturated soil conditions prevail. Interestingly, despite the small changes of post-fire DOC concentrations relative to pre-fire levels (Figure 5, Supplementary Figure S2), we do not observe a significant correlation between Al and DOC in the three catchments after fire (data not shown).

Spectroscopic data show slight changes in the molecular structure of dissolved organic matter (DOM) in the streams of the JRB-CZO headwaters after burning (Figure 7). Increased fluorescence indices (FI values) of DOM in the surface waters of the three catchments suggests a decrease in prevalence of plant-derived DOM due to biomass combustion (Olshansky et al., 2018a). Moreover, increased HIX values in streams after fire could be the result of pyrogenic carbon (PyC) production and dissolution (Roebuck et al., 2018; Jones et al., 2019). However, we also observed a decrease in SUVA, which suggests a decrease, rather than an increase, in aromatic DOM (Birdwell and Engel, 2010). Small, more polar, and less polycondensed aromatic structures of PyC have a higher aqueous solubility relative to larger and highly condensed molecules (Wagner et al., 2017). Additionally, when exposed to light, highly aromatic PyC is prone to photo-degradation producing smaller N-rich aliphatic molecules (Bostick et al., 2020; Goranov et al., 2020), which could explain the decrease in SUVA. The role of metal complexation with dissolved pyrogenic carbon remains poorly understood (Wagner et al., 2017), but it is feasible that Al complexation with photo-chemically transformed PyC may not be favored, as N-containing functional groups form less stable metal complexes than do those functional groups containing carboxylic and phenolic oxygen (Vance et al., 1996). Additionally, given that we did not observe a significant difference between pre- and post-fire Si concentrations and VWMs, it is possible that enhanced incongruent weathering after fire could have led to the retention of Al and Fe in the system. These observations, nevertheless, should be treated with care as further research must be conducted, e.g., column experiments, to examine the relationships between pyrogenic carbon and the solubilization and mobilization of polyvalent cations, e.g., Al and Fe, in combusted soils.

### 4.3. Soils control post-fire solute exports

Wildfires have a direct impact on forest floors and soil biogeochemical processes, which can alter soil solution chemistry for extended periods of time (Chorover et al., 1994; Williams and Melack, 1997b; Rhoades et al., 2011, 2019). These fire-induced pore water solute concentrations can rapidly propagate

through the surface and subsurface to the streams and may drive the observed responses of solute concentrations and fluxes of the three headwater catchments in the JRB-CZO after the fire. Although, groundwater dominates streamflow generation in the JRB-CZO (Liu et al., 2008b; Zapata-Rios et al., 2015; McIntosh et al., 2017; White et al., 2019, 2021), shallow subsurface lateral flow contributions are intensified during wet seasons (i.e., spring snowmelt) (McIntosh et al., 2017; White et al., 2021). Moreover, the tight hydraulic connectivity among soil water, shallow and deep groundwater, and surface water in the JRB-CZO (Olshansky et al., 2018b; White et al., 2019) facilitates the quick transfer of solutes from soils to the groundwater and streams.

Similarly, studies in forested watersheds have shown nutrient ion concentrations in surface waters reflect the chemical signature of soils during snowmelt (Williams and Melack, 1991; Brooks et al., 1999). Furthermore, clockwise hysteresis of non-hydrolyzing cations ( $\text{Ca}^{2+}$ ,  $\text{Mg}^{2+}$ , and  $\text{K}^{+}$ ) and strong acid anions ( $\text{NO}_3^-$  and  $\text{SO}_4^{2-}$ ) during peak flows in La Jara surface waters suggests flush of these ions from soil surfaces to the streams (Olshansky et al., 2018b). Hydrologic and geochemical connections from soils to streams are such that during periods of soil saturation, suspended and dissolved materials—from long term ash deposits on hillslopes, alluvial fans, and valley bottoms—may not only be flushed from the soil upper horizons to the stream, but also may be transported downward into the vadose zone. These partitioning processes, therefore, may increase the stores and residence times of fire-derived solutes in burned watersheds, maintaining concentrations higher than background levels for extended periods of time post-fire. Nevertheless, fire recovery—e.g., vegetation regrowth, biotic uptake—play an important role on the system resiliency of post-fire solute exports in the long term (Figures 6, 8).

Further evidence of the direct influence of post-fire soil chemical signatures on stream waters in the JRB-CZO is observed in the surface water solute concentrations of the ZOB—nested within La Jara catchment—after the fire. The ZOB surface waters are a proxy for soil solution, with only very shallow groundwater contributions (Perdrial et al., 2014; Olshansky et al., 2018b). Nutrient anion (i.e.,  $\text{NO}_3^-$ ,  $\text{Cl}^-$ , and  $\text{SO}_4^{2-}$ ) and cation (e.g.,  $\text{Ca}^{2+}$ ,  $\text{Mg}^{2+}$ , and  $\text{K}^{+}$ ) concentrations in the ZOB (Supplementary Figure S3) mimicked those patterns observed at the outlets of La Jara, History Grove, and Upper Jaramillo catchments after the fire. This result suggests again the tight influence of the post-fire soil biogeochemical processes in the headwaters in the JRB-CZO solute effluxes.

## 5. Conclusions

Our results demonstrate the close relationship between soil physical and biogeochemical processes and catchment solute mobilization and exports after wildfires. We observed increased surface water runoff and stream water solute concentrations and fluxes after fire compared to pre-fire baselines. After the initial post-fire solute pulse, base cation ( $\text{Ca}^{2+}$  and  $\text{Mg}^{2+}$ ) strong acid anion ( $\text{NO}_3^-$  and  $\text{SO}_4^{2-}$ ) concentrations remained above pre-burn baselines throughout the full duration of the study. We hypothesize that enhanced transport of

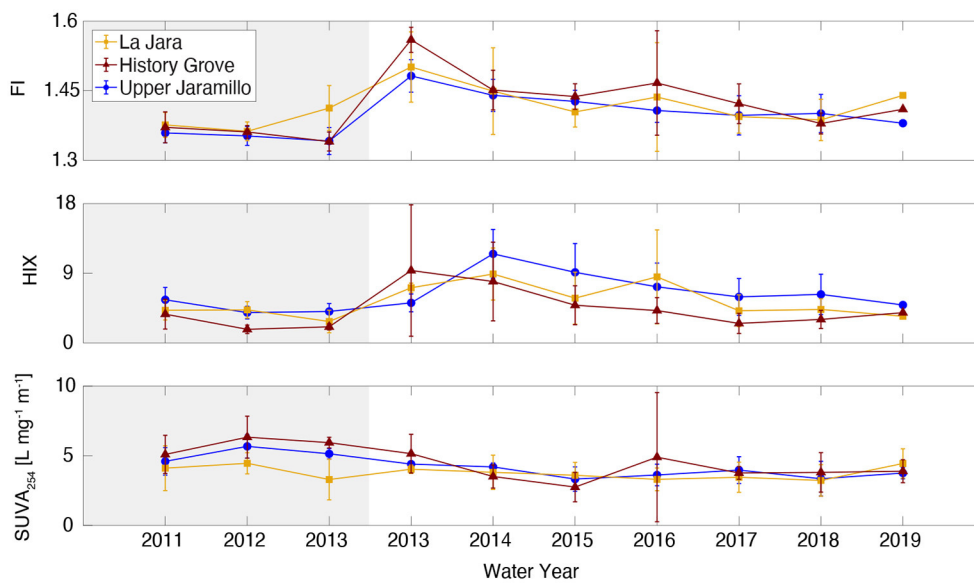


**FIGURE 7**  
Annual volume-weighted means (VWM) of the fluorescence Index (FI), humification index (HIX) and specific UV absorbance at 245 nm (SUVA<sub>254</sub>), from La Jara, History Grove, and Upper Jaramillo catchments. Notice that for the WY 2013 there are two calculated fluxes—before and after the Thompson Ridge Wildfire in the summer of 2013—in order to illustrate the immediate effect of the fire in the three headwater catchments.

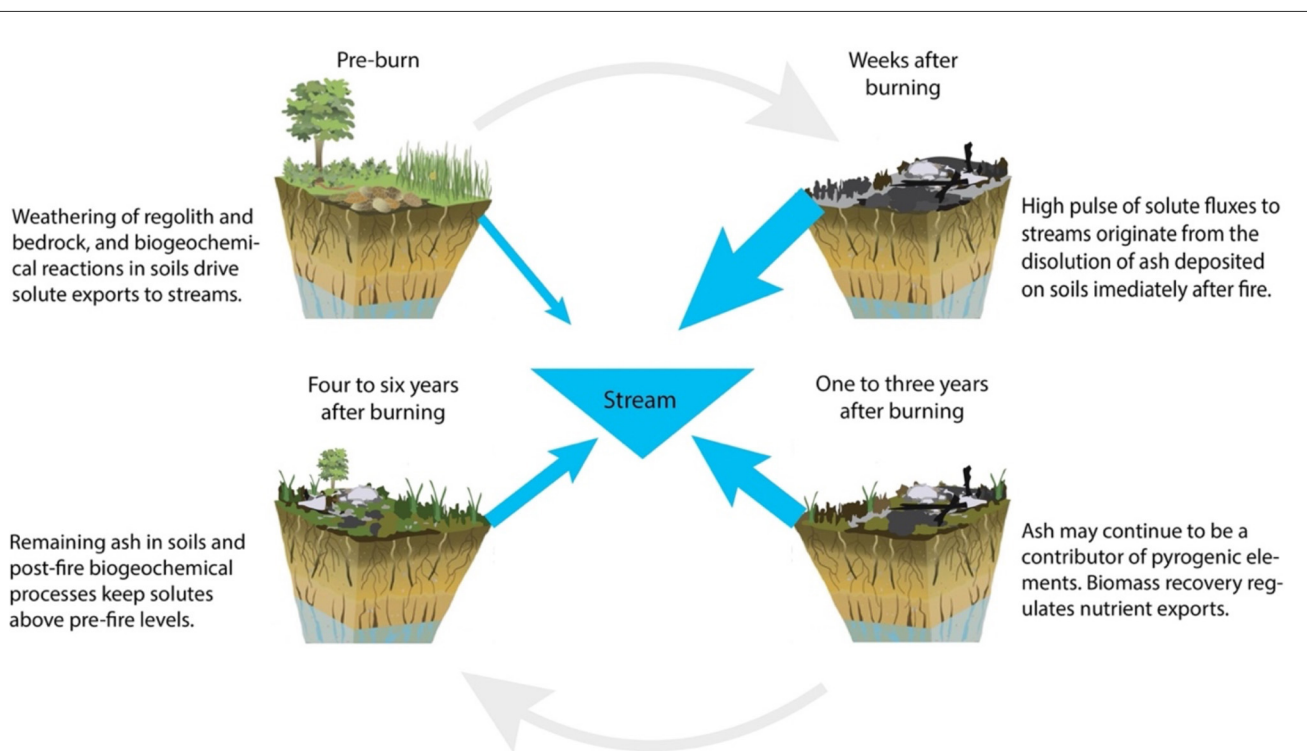


**FIGURE 8**  
Conceptual model of evolution of solute exports after fire. Blue arrows represent the magnitude of solute mobilization in the three periods after burning—a few weeks after fire, 1–3 years after fire, and 4–6 years post-burn. Figure modified from [Chorover et al. \(2007\)](#).

suspended sediments and solutes, their retardation during transport (e.g., in the vadose zone) and the progressive evolution of soil biogeochemical processes after fires may be the main drivers for sustaining the elevated level of chemical

denudation of the burned forested catchment for several years post-fire.

Moreover, despite the small changes in DOC concentration pre- and post-fire, the molecular structure of DOM was altered as a

result of the fire, and this impacted surface water concentrations of DOM-complexing polyvalent cations (e.g., Al and Fe). The latter decreased significantly post-fire, particularly during periods of soil saturation (e.g., snowmelt and monsoon seasons) when high fluxes from soils to streams were expected. Considering that the transport mechanisms of these metals is *via* complexation with organic matter and/or as mobile colloids, our observations suggest that changes in organic matter composition after fire (e.g., increased HIX) and the presence of PyC may inhibit metal complexation. Better characterization of the physical and chemical properties of combusted organic matter will shed light in the possible mechanisms controlling mobilization/retention of polyvalent cations in burned soils. Nonetheless, these observations strengthen the hypothesis of the importance of soil processes in solute mobilization through the critical zone after wildfires.

As this work was conducted over a decade with pre- and post-burn fire data collected on three distinct catchments, we can conclude that fire intensity, burn size and catchment hydrology all contribute to the long-term solute flux post-fire response. Longer water residence times in the predominantly north-facing slopes of Upper Jaramillo catchment (Broxton et al., 2009) lengthened the observed post-fire solute losses. Conversely, the flashy La Jara and History Grove streams more rapidly mobilized solutes post-fire. More importantly, burn severity drives solute flux amplitudes. La Jara and History Grove catchments, which were subject to higher burn severity, exhibited greater solute efflux above pre-burn baseline than did the less severely burn Upper Jaramillo catchment. Moreover, despite these differences, toward the end of the post-fire period these surface waters presented low and similar solute effluxes, indicating the ca. 6 year time-scale of system recovery.

This study highlights the fact that wildfires can play a significant role in the pulsed release of lithogenic solutes and hence landscape chemical denudation. While rock weathering products accumulate over the course of biomass accretion, biomass combustion results in their pulsed release to effluent stream waters. Hence, forest biomass can be viewed as a temporary store for catchment solute effluxes. Post-fire, these solutes are retarded to varying degrees during transport through soil and regolith. Although western montane ecosystems have evolved with wildfire as a natural disturbance, increases in fire frequency, intensity and size that accompany climate change superimposed with the high fuel loads promoted by a century of fire suppression, may jeopardize the quality of water emanating from forested catchments for extended periods of times, especially in semi-arid region where fresh water sources are scarce. This in turn represents a hurdle to water managers when locating safe fresh water sources for human consumption that meet the performance standards of the existing conventional water treatments plants.

## Data availability statement

The datasets presented in this study can be found in online repositories. The names of the repository/repositories and accession number(s) can be found in the article/Supplementary material.

## Author contributions

RS performed the data analysis, developed the conceptual framework, and wrote the manuscript with support from TM, TR, PF, MW, and JC. TM and JC supervised the project. All authors contributed to the article and approved the submitted version.

## Funding

This research was funded by the National Science Foundation, grant numbers EAR-0724958, EAR-1331408, and EAR-2012123.

## Acknowledgments

We dedicate this paper in memory of the second author, TM, for his significant and far-reaching contributions to watershed biogeochemistry research. Under his motto making the world better through biogeochemistry, his selfless commitment to research and teaching was an inspiration to his peers and countless students he advised during his career. TM was a cherished mentor, colleague, and friend who brought warmth, humor, and kindness to every work place he belonged to and will be deeply missed by all who had the privilege of knowing and working with him. The authors would like to thank the research group of the Catalina-Jemez Critical Zone Observatory of the University of Arizona. All data utilized in this paper are available through the [criticalzone.org](http://criticalzone.org) website at <http://criticalzone.org/catalina-jemez/data/>.

## In memoriam

This paper is dedicated to the memory of TM who passed away on October 5, 2022.

## Conflict of interest

The authors declare that the research was conducted in the absence of any commercial or financial relationships that could be construed as a potential conflict of interest.

## Publisher's note

All claims expressed in this article are solely those of the authors and do not necessarily represent those of their affiliated organizations, or those of the publisher, the editors and the reviewers. Any product that may be evaluated in this article, or claim that may be made by its manufacturer, is not guaranteed or endorsed by the publisher.

## Supplementary material

The Supplementary Material for this article can be found online at: <https://www.frontiersin.org/articles/10.3389/frwa.2023.1148298/full#supplementary-material>

## References

- Ackley, C., Tank, S. E., Haynes, K. M., Rezanezhad, F., McCarter, C., and Quinton, W. L. (2021). Coupled hydrological and geochemical impacts of wildfire in peatland-dominated regions of discontinuous permafrost. *Sci. Total Environ.* 782, 146841. doi: 10.1016/j.scitotenv.2021.146841
- Allison, R. J., and Bristow, G. E. (1999). The effects of fire on rock weathering: some further considerations of laboratory experimental simulation. *Earth Surf. Process. Landf.* 24, 707–713. doi: 10.1002/(SICI)1096-9837(199908)24:8<707::AID-ESP993>3.0.CO;2-Z
- Araya, S. N., Meding, M., and Berhe, A. A. (2016). Thermal alteration of soil physico-chemical properties: a systematic study to infer response of Sierra Nevada climate sequence soils to forest fires. *Soil.* 2, 351–366. doi: 10.5194/soil-2-351-2016
- Bayley, S. E., Schindler, D. W., Beaty, K. G., Parker, B. R., and Stainton, M. P. (1992a). Effects of multiple fires on nutrient yields from streams draining boreal forest and fen watersheds: nitrogen and phosphorus. *Can. J. Fish. Aquat. Sci.* 49, 584–596. doi: 10.1139/f92-068
- Bayley, S. E., Schindler, D. W., Parker, B. R., Stainton, M. P., and Beaty, K. G. (1992b). Effects of forest fire and drought on acidity of a base-poor boreal forest stream: similarities between climatic warming and acidic precipitation. *Biogeochemistry.* 17, 191–204. doi: 10.1007/BF00004041
- Birdwell, J. E., and Engel, A. S. (2010). Characterization of dissolved organic matter in cave and spring waters using UV-Vis absorbance and fluorescence spectroscopy. *Org. Geochem.* 41, 270–280. doi: 10.1016/j.orggeochem.2009.11.002
- Blake, W. H., Wallbrink, P. J., and Droppo, I. G. (2009). Sediment aggregation and water quality in wildfire-affected river basins. *Mar. Freshw. Res.* 60, 653–659. doi: 10.1071/MF08068
- Bodi, M. B., Martin, D. A., Balfour, V. N., Santin, C., Doerr, S. H., Pereira, P., et al. (2014). Wildland fire ash: Production, composition and eco-hydro-geomorphic effects. *Earth-Sci. Rev.* 130, 103–127. doi: 10.1016/j.earscirev.2013.12.007
- Bostick, K. W., Zimmerman, A. R., Goranov, A. I., Mitra, S., Hatcher, P. G., and Wozniak, A. S. (2020). Photolability of pyrogenic dissolved organic matter from a thermal series of laboratory-prepared chars. *Sci. Total Environ.* 724, 138198. doi: 10.1016/j.scitotenv.2020.138198
- Brooks, P. D., McKnight, D. M., and Bencala, K. E. (1999). The relationship between soil heterotrophic activity, soil dissolved organic carbon (DOC) leachate, and catchment-scale DOC export in headwater catchments. *Water Resour. Res.* 35, 1895–1902. doi: 10.1029/1998WR900125
- Broxton, P. D., Harpold, A. A., Biederman, J. A., Troch, P. A., Molotch, N. P., and Brooks, P. D. (2015). Quantifying the effects of vegetation structure on snow accumulation and ablation in mixed-conifer forests. *Ecohydrology.* 8, 1073–1094. doi: 10.1002/eco.1565
- Broxton, P. D., Troch, P. A., and Lyon, S. W. (2009). On the role of aspect to quantify water transit times in small mountainous catchments. *Water Res. Res.* 45, 8. doi: 10.1029/2008WR007438
- Buckman, S., Morris, R. H., and Bourman, R. P. (2021). Fire-induced rock spalling as a mechanism of weathering responsible for flared slope and inselberg development. *Nat. Commun.* 12, 2150. doi: 10.1038/s41467-021-22451-2
- Cerrato, J. M., Blake, J. M., Hirani, C., Clark, A. L., Ali, A.-M. S., Artyushkova, K., et al. (2016). Wildfires and water chemistry: effect of metals associated with wood ash. *Environ. Sci.: Process. Impacts.* 18, 1078–1089. doi: 10.1039/C6EM00123H
- Chipera, S. J., Goff, F., Goff, C. J., and Fittipaldo, M. (2008). Zeolitization of intracaldera sediments and rhyolitic rocks in the 1.25 Ma lake of Valles caldera, New Mexico, USA. *J. Volcanol. Geotherm. Res.* 178, 317–330. doi: 10.1016/j.jvolgeores.2008.06.032
- Chorover, J., Kretzschmar, R., Garcia-Pichel, F., and Sparks, D. L. (2007). Soil biogeochemical processes within the critical zone. *Elements.* 3, 321–326. doi: 10.2113/gselements.3.5.321
- Chorover, J., Vitousek, P. M., Everson, D. A., Esperanza, A. M., and Turner, D. (1994). Solution chemistry profiles of mixed-conifer forests before and after fire. *Biogeochemistry.* 26, 115–144. doi: 10.1007/BF02182882
- Clark, K. L., Skowronski, N., Gallagher, M., Renninger, H., and Schäfer, K. (2012). Effects of invasive insects and fire on forest energy exchange and evapotranspiration in the New Jersey pinelands. *Agric. For. Meteorol.* 166–167, 50–61. doi: 10.1016/j.agrformet.2012.07.007
- DeBano, L. F. (2000). The role of fire and soil heating on water repellency in wildland environments: a review. *J. Hydrology.* 231–232, 195–206. doi: 10.1016/S0022-1694(00)00194-3
- Demuth, H., Beale, M., and Hagan, M. (1994). *Neural Network Toolbox*. Available online at: <https://www.fsb.unizg.hr/hydro/bib/books/Neural%20Network%20Toolbox%20MATHLAB.pdf> (accessed March, 2022).
- Eidenshink, J., Schwind, B., Brewer, K., Zhu, Z.-L., Quayle, B., and Howard, S. (2007). A project for monitoring trends in burn severity. *Fire Ecol.* 3, 3–21. doi: 10.4996/fireecology.0301003
- Engle, D. L., Sickman, J. O., Moore, C. M., Esperanza, A. M., Melack, J. M., and Keeley, J. E. (2008). Biogeochemical legacy of prescribed fire in a giant sequoia-mixed conifer forest: A 16-year record of watershed balances. *J. Geophys. Res.* 113, G1. doi: 10.1029/2006JG000391
- Gallet, C., and Pellissier, F. (1997). Phenolic compounds in natural solutions of a coniferous forest. *J. Chem. Ecol.* 23, 2401–2412. doi: 10.1023/B:JOEC.0000006682.50061.83
- Godsey, S. E., Kirchner, J. W., and Clow, D. W. (2009). Concentration–discharge relationships reflect chemostatic characteristics of US catchments. *Hydrol. Process.* 23, 1844–1864. doi: 10.1002/hyp.7315
- Goff, F., Gardner, J. N., Reneau, S. L., Kelley, S. A., Kempton, K. A., and Lawrence, J. R. (2011). “Geologic map of the Valles caldera, Jemez Mountains, New Mexico,” in *New Mexico Bur Geol Min Res Geol Map*. p. 79. Available online at: [https://geoinfo.nmt.edu/repository/data/2011/20110002/GM-79\\_booklet.pdf](https://geoinfo.nmt.edu/repository/data/2011/20110002/GM-79_booklet.pdf) (accessed March, 2021).
- Goranov, A. I., Wozniak, A. S., Bostick, K. W., Zimmerman, A. R., Mitra, S., and Hatcher, P. G. (2020). Photochemistry after fire: structural transformations of pyrogenic dissolved organic matter elucidated by advanced analytical techniques. *Geochim. Cosmochim. Acta.* 290, 271–292. doi: 10.1016/j.gca.2020.08.030
- Goudie, A. S., Allison, R. J., and McLaren, S. J. (1992). The relations between modulus of elasticity and temperature in the context of the experimental simulation of rock weathering by fire. *Earth Surf. Process. Landf.* 17, 605–615. doi: 10.1002/esp.3290170606
- Goulden, M. L., and Bales, R. C. (2019). California forest die-off linked to multi-year deep soil drying in 2012–2015 drought. *Nat. Geosci.* 12, 632–637. doi: 10.1038/s41561-019-0388-5
- Granath, G., Evans, C. D., Strengbom, J., Fölster, J., Grelle, A., Strömquist, J., et al. (2021). The impact of wildfire on biogeochemical fluxes and water quality in boreal catchments. *Biogeosciences.* 18, 3243–3261. doi: 10.5194/bg-18-3243-2021
- Gustavsson, M., Karlsson, S., Oberg, G., Sandén, P., Svensson, T., Valinia, S., et al. (2012). Organic matter chlorination rates in different boreal soils: the role of soil organic matter content. *Environ. Sci. Technol.* 46, 1504–1510. doi: 10.1021/es203191r
- Gustine, R. N., Hanan, E. J., Robichaud, P. R., and Elliot, W. J. (2022). From burned slopes to streams: how wildfire affects nitrogen cycling and retention in forests and fire-prone watersheds. *Biogeochemistry.* 157, 51–68. doi: 10.1007/s10533-021-00861-0
- Harpold, A. A., Biederman, J. A., Condon, K., Merino, M., Korgaonkar, Y., Nan, T., et al. (2014). Changes in snow accumulation and ablation following the Las Conchas Forest Fire, New Mexico, USA: changes in snow following fire. *Ecohydrology.* 7, 440–452. doi: 10.1002/eco.1363
- Harvey, C. L., Dixon, H., and Hannaford, J. (2012). An appraisal of the performance of data-infilling methods for application to daily mean river flow records in the UK. *Hydrology Res.* 43, 618–636. doi: 10.2166/nh.2012.110
- Hernández, T., García, C., and Reinhardt, I. (1997). Short-term effect of wildfire on the chemical, biochemical and microbiological properties of Mediterranean pine forest soils. *Biol. Fertil. Soils* 25, 109–116. doi: 10.1007/s003740050289
- Humphreys, G. S., Shakesby, R. A., Doerr, S. H., Blake, W. H., Wallbrink, P., and Hart, D. M. (2003). “Some effects of fire on the regolith,” in *Advances in Regolith*. p. 216–220.
- Ilunga, M., and Stephenson, D. (2005). Infilling streamflow data using feed-forward back-propagation (BP) artificial neural networks: Application of standard BP and pseudo Mac Laurin power series BP techniques. *Water.* 31, 171–176. doi: 10.4314/wsa.v31i2.5199
- Jones, M. W., Aragão, L. E. O. C., Dittmar, T., Rezende, C. E., Almeida, M. G., Johnson, B. T., et al. (2019). Environmental controls on the riverine export of dissolved black carbon. *Global Biogeochem. Cycles.* 33, 849–874. doi: 10.1029/2018GB006140
- Jung, H. Y., Hogue, T. S., Rademacher, L. K., and Meixner, T. (2009). Impact of wildfire on source water contributions in devil creek, CA: evidence from end-member mixing analysis. *Hydrol. Process.* 23, 183–200. doi: 10.1002/hyp.7132
- Kim, J.-W., and Pachepsky, Y. A. (2010). Reconstructing missing daily precipitation data using regression trees and artificial neural networks for SWAT streamflow simulation. *J. Hydrol.* 394, 305–314. doi: 10.1016/j.jhydrol.2010.09.005
- Kişi Özgür (2007). Streamflow Forecasting Using Different Artificial Neural Network Algorithms. *J. Hydrol. Eng.* 12, 532–539. doi: 10.1061/(ASCE)1084-0699(2007)12:5(532)
- Kramer, P. (2012). *Physiology of Woody Plants*. Amsterdam, Netherlands: Elsevier.
- Kunze, M. D., and Stednick, J. D. (2006). Streamflow and suspended sediment yield following the 2000 Bobcat fire, Colorado. *Hydrol. Process.* 20, 1661–1681. doi: 10.1002/hyp.5954
- Liang, B., Lehmann, J., Solomon, D., Kinyangi, J., Grossman, J., O'Neill, B., et al. (2006). Black carbon increases cation exchange capacity in soils. *Soil Sci. Soc. Am. J.* 70, 1719. doi: 10.2136/sssaj2005.0383

- Liu, F., Bales, R. C., Conklin, M. H., and Conrad, M. E. (2008a). Streamflow generation from snowmelt in semi-arid, seasonally snow-covered, forested catchments, Valles Caldera, New Mexico: streamflow generation in Valles Caldera. *Water Resour. Res.* 44, 12. doi: 10.1029/2007WR006728
- Liu, F., Parmenter, R., Brooks, P. D., Conklin, M. H., and Bales, R. C. (2008b). Seasonal and interannual variation of streamflow pathways and biogeochemical implications in semi-arid, forested catchments in Valles Caldera, New Mexico. *Ecohydrology*. 1, 239–252. doi: 10.1002/eco.22
- Lyon, S. W., Troch, P. A., Broxton, P. D., Molotch, N. P., and Brooks, P. D. (2008). Monitoring the timing of snowmelt and the initiation of streamflow using a distributed network of temperature/light sensors. *Ecohydrology*. 1, 215–224. doi: 10.1002/eco.18
- Maina, F. Z., and Siirila-Woodburn, E. R. (2020). Watersheds dynamics following wildfires: Nonlinear feedbacks and implications on hydrologic responses. *Hydrol. Process.* 34, 33–50. doi: 10.1002/hyp.13568
- Mast, M. A., and Clow, D. W. (2008). Effects of 2003 wildfires on stream chemistry in Glacier National Park, Montana. *Hydrol. Process.* 22, 5013–5023. doi: 10.1002/hyp.7121
- McIntosh, J., Chorover, J., Troch, P., Brooks, P., Amistadi, M. K., Corley, T., et al. (2021). CJCZO–Stream Water Chemistry–Jemez River Basin–(2005–2020), *HydroShare*. Available online at: <http://www.hydroshare.org/resource/553c42d3a8ee40309b2d77071aa25f2e>
- McIntosh, J. C., Schaumberg, C., Perdrial, J., Harpold, A., Vázquez-Ortega, A., Rasmussen, C., et al. (2017). Geochemical evolution of the Critical Zone across variable time scales informs concentration-discharge relationships: Jemez River Basin Critical Zone Observatory: EVOLUTION OF CZ informs C-Q RELATIONS. *Water Resour. Res.* 53, 4169–4196. doi: 10.1002/2016WR019712
- Meixner, T., Shaw, J. R., and Bales, R. C. (2004). Temporal and spatial variability of cation and silica export in an alpine watershed, Emerald Lake, California. *Hydrol. Process.* 18, 1759–1776. doi: 10.1002/hyp.1416
- Montelius, M., Thiry, Y., Marang, L., Ranger, J., Cornelis, J.-T., Svensson, T., et al. (2015). Experimental evidence of large changes in terrestrial chlorine cycling following altered tree species composition. *Environ. Sci. Technol.* 49, 4921–4928. doi: 10.1021/acs.est.5b00137
- Moravec, B. G., White, A. M., Root, R. A., Sanchez, A., Olshansky, Y., Paras, B. K., et al. (2020). Resolving deep critical zone architecture in complex volcanic terrain. *J. Geophys. Res.* 125, 20–21. doi: 10.1029/2019JF005189
- Moré, J. J. (1978). The levenberg-marquardt algorithm: implementation and theory. *Num. Anal.* 105–116. doi: 10.1007/BFb0067700
- Murphy, J. D., Johnson, D. W., Miller, W. W., Walker, R. F., Carroll, E. F., and Blank, R. R. (2006). Wildfire effects on soil nutrients and leaching in a tahoe basin watershed. *J. Environ. Qual.* 35, 479–489. doi: 10.2134/jeq2005.0144
- Musselman, K. N., Molotch, N. P., and Brooks, P. D. (2008). Effects of vegetation on snow accumulation and ablation in a mid-latitude sub-alpine forest. *Hydrol. Process.* 22, 2767–2776. doi: 10.1002/hyp.7050
- Näthe, K., Levia, D. F., Tischer, A., and Potthast, K. (2018). Spatiotemporal variation of aluminium and micro-and macronutrients in the soil solution of a coniferous forest after low-intensity prescribed surface fires. *Int. J. Wildland Fire.* 27, 471–489. doi: 10.1071/WF17178
- Nielson, D. L., and Hulen, J. B. (1984). Internal geology and evolution of the Redondo Dome, Valles Caldera, New Mexico. *J. Geophys. Res.* 89, 8695. doi: 10.1002/9781118782095.ch33
- Olshansky, Y., Root, R. A., and Chorover, J. (2018a). Wet–dry cycles impact DOM retention in subsurface soils. *Biogeosciences*. 15, 821–832. doi: 10.5194/bg-15-821-2018
- Olshansky, Y., White, A. M., Moravec, B. G., McIntosh, J., and Chorover, J. (2018b). Subsurface pore water contributions to stream concentration-discharge relations across a snowmelt hydrograph. *Front. Earth Sci.* 6, 181. doi: 10.3389/feart.2018.00181
- Orem, C. A., and Pelletier, J. D. (2016). The predominance of post-wildfire erosion in the long-term denudation of the Valles Caldera, New Mexico. *J. Geophys. Res.* 121, 843–864. doi: 10.1002/2015JF003663
- Perdrial, J. N., McIntosh, J., Harpold, A., Brooks, P. D., Zapata-Rios, X., Ray, J., et al. (2014). Stream water carbon controls in seasonally snow-covered mountain catchments: impact of inter-annual variability of water fluxes, catchment aspect and seasonal processes. *Biogeochemistry*. 118, 273–290. doi: 10.1007/s10533-013-9929-y
- Pereira, P., Úbeda, X., Martin, D., Mataix-Solera, J., Cerdà, A., and Burguet, M. (2014). Wildfire effects on extractable elements in ash from a Pinus pinaster forest in Portugal. *Hydrol. Process.* 28, 3681–3690. doi: 10.1002/hyp.9907
- Pereira, P., Úbeda, X., and Martin, D. A. (2012). Fire severity effects on ash chemical composition and water-extractable elements. *Geoderma*. 191, 105–114. doi: 10.1016/j.geoderma.2012.02.005
- Petty, T. R., and Dhingra, P. (2018). Streamflow hydrology estimate using machine learning (SHEM). *J. Am. Water Resour. Assoc.* 54, 55–68. doi: 10.1111/1752-1688.12555
- Potthast, K., Meyer, S., Creclius, A. C., Schubert, U. S., Tischer, A., and Michalzik, B. (2017). Land-use and fire drive temporal patterns of soil solution chemistry and nutrient fluxes. *Sci. Total Environ.* 605–606, 514–526. doi: 10.1016/j.scitotenv.2017.06.182
- Quill, E. S., Angove, M. J., Morton, D. W., and Johnson, B. B. (2010). Characterisation of dissolved organic matter in water extracts of thermally altered plant species found in box–ironbark forests. *Soil Res.* 48, 693–704. doi: 10.1071/SR09157
- Reneau, S. L., Katzman, D., Kuyumjian, G. A., Lavine, A., and Malmon, D. V. (2007). Sediment delivery after a wildfire. *Geology*. 35, 151–154. doi: 10.1130/G23288A.1
- Rhoades, C. C., Entwistle, D., and Butler, D. (2011). The influence of wildfire extent and severity on streamwater chemistry, sediment and temperature following the Hayman Fire, Colorado. *Int. J. Wildland Fire.* 20, 430–442. doi: 10.1071/WF09086
- Rhoades, C. C., Nunes, J. P., Silins, U., and Doerr, S. H. (2019). The influence of wildfire on water quality and watershed processes: new insights and remaining challenges. *Int. J. Wildland Fire.* 28, 721–725. doi: 10.1071/WFv28n10\_FO
- Roebuck, J. A., Medeiros, P. M., Letourneau, M. L., and Jaffé, R. (2018). Hydrological controls on the seasonal variability of dissolved and particulate black carbon in the Altamaha river, GA. *J. Geophysical Res.* 123, 3055–3071. doi: 10.1029/2018JG004406
- Rust, A. J., Hogue, T. S., Saxe, S., and McCray, J. (2018). Post-fire water-quality response in the western United States. *Int. J. Wildland Fire.* 27, 203–216. doi: 10.1071/WF17115
- Santos, F., Wymore, A. S., Jackson, B. K., Sullivan, S. M. P., McDowell, W. H., and Berhe, A. A. (2019). Fire severity, time since fire, and site-level characteristics influence streamwater chemistry at baseflow conditions in catchments of the Sierra Nevada, California, USA. *Fire Ecol.* 15, 3. doi: 10.1186/s42408-018-0022-8
- Shakesby, R. A., and Doerr, S. H. (2006). Wildfire as a hydrological and geomorphological agent. *Earth-Sci. Rev.* 74, 269–307. doi: 10.1016/j.earscirev.2005.10.006
- Shiau, J.-T., and Hsu, H.-T. (2016). Suitability of ANN-based daily streamflow extension models: a case study of gaoping river basin, Taiwan. *Water Res. Manag.* 30, 1499–1513. doi: 10.1007/s11269-016-1235-8
- Shindo, H., and Kuwatsuka, S. (1977). Behavior of phenolic substances in the decaying process of plants. *Soil Sci. Plant Nutr.* 23, 185–193. doi: 10.1080/00380768.1977.10433035
- Shtober-Zisu, N., Tessler, N., Tsatskin, A., and Greenbaum, N. (2015). Accelerated weathering of carbonate rocks following the 2010 wildfire on Mount Carmel, Israel. *Int. J. Wildland Fire.* 24, 1154–1167. doi: 10.1071/WF14221
- Shtober-Zisu, N., and Wittenberg, L. (2021). Long-term effects of wildfire on rock weathering and soil stoniness in the Mediterranean landscapes. *Sci. Total Environ.* 762, 143125. doi: 10.1016/j.scitotenv.2020.143125
- Smith, H. G., Sheridan, G. J., Lane, P. N. J., Nyman, P., and Haydon, S. (2011). Wildfire effects on water quality in forest catchments: a review with implications for water supply. *J. Hydrol.* 396, 170–192. doi: 10.1016/j.jhydrol.2010.10.043
- Smith, H. G., Sheridan, G. J., Nyman, P., Child, D. P., Lane, P. N. J., Hotchkis, M. A. C., et al. (2012). Quantifying sources of fine sediment supplied to post-fire debris flows using fallout radionuclide tracers. *Geomorphology*. 139–140, 403–415. doi: 10.1016/j.geomorph.2011.11.005
- Stephens, S. L., Meixner, T., Poth, M., McGurk, B., and Payne, D. (2004). Prescribed fire, soils, and stream water chemistry in a watershed in the Lake Tahoe Basin, California. *Int. J. Wildland Fire.* 13, 27–35. doi: 10.1071/WF03002
- Svensson, T., Kylin, H., Montelius, M., Sandén, P., and Bastviken, D. (2021). Chlorine cycling and the fate of Cl in terrestrial environments. *Environ. Sci. Pollut. Res. Int.* 28, 7691–7709. doi: 10.1007/s11356-020-12144-6
- Swindle, C., Shankin-Clarke, P., Meyerhof, M., Carlson, J., and Melack, J. (2021). Effects of wildfires and ash leaching on stream chemistry in the Santa Ynez mountains of Southern California. *Water*. 13, 2402. doi: 10.3390/w13172402
- Trostle, K. D., Ray Runyon, J., Pohlmann, M. A., Redfield, S. E., Pelletier, J., McIntosh, J., et al. (2016). Colloids and organic matter complexation control trace metal concentration-discharge relationships in Marshall Gulch stream waters. *Water Resour. Res.* 52, 7931–7944. doi: 10.1002/2016WR019072
- Vance, G. F., Mokma, D. L., and Boyd, S. A. (1986). Phenolic compounds in soils of hydrosequences and developmental sequences of spodosols. *Soil Sci. Soc. Am. J.* 50, 992–996. doi: 10.2136/sssaj1986.03615995005000040032x
- Vance, G. F., Stevenson, F. J., and Sikora, F. J. (1996). “Environmental chemistry of aluminum-organic complexes,” in *The Environmental Chemistry of Aluminum*. p. 2.
- Vázquez-Ortega, A., Perdrial, J., Harpold, A., Zapata-Rios, X., Rasmussen, C., McIntosh, J., et al. (2015). Rare earth elements as reactive tracers of biogeochemical weathering in forested rhyolitic terrain. *Chem. Geol.* 391, 19–32. doi: 10.1016/j.chemgeo.2014.10.016
- Vodyanitskii, Y. N., and Makarov, M. I. (2017). Organochlorine compounds and the biogeochemical cycle of chlorine in soils: a review. *Eurasian Soil Sci.* 50, 1025–1032. doi: 10.1134/S1064229317090113
- Wagner, S., Ding, Y., and Jaffé, R. (2017). A new perspective on the apparent solubility of dissolved black carbon. *Front. Earth Sci. China.* 5, 00075. doi: 10.3389/feart.2017.00075

- White, A., Ma, L., Moravec, B., Chorover, J., and McIntosh, J. (2021). U-series and Sr isotopes as tracers of mineral weathering and water routing from the deep Critical Zone to streamflow in a high-elevation volcanic catchment. *Chem. Geol.* 570, 120156. doi: 10.1016/j.chemgeo.2021.120156
- White, A., Moravec, B., McIntosh, J., Olshansky, Y., Paras, B., Sanchez, R. A., et al. (2019). Distinct stores and the routing of water in the deep critical zone of a snow-dominated volcanic catchment. *Hydrol. Earth Syst. Sci.* 23, 4661–4683. doi: 10.5194/hess-23-4661-2019
- Williams, M. R., and Melack, J. M. (1997a). Atmospheric deposition, mass balances, and processes regulating streamwater solute concentrations in mixed-conifer catchments of the Sierra Nevada, California. *Biogeochemistry*. 37, 111–144.
- Williams, M. R., and Melack, J. M. (1997b). Effects of prescribed burning and drought on the solute chemistry of mixed-conifer forest streams of the Sierra Nevada, California. *Biogeochemistry*. 39, 225–253.
- Williams, M. W., and Melack, J. M. (1991). Solute chemistry of snowmelt and runoff in an Alpine Basin, Sierra Nevada. *Water Resour. Res.* 27, 1575–1588. doi: 10.1029/90WR02774
- Wolff, J. A., Brunstad, K. A., and Gardner, J. N. (2011). Reconstruction of most recent volcanic eruptions from the Valles caldera, New Mexico. *J. Volcanol. Geothermal Res.* 199, 53–68. doi: 10.1016/j.jvolgeores.2010.10.008
- Wu, C. L., and Chau, K. W. (2010). Data-driven models for monthly streamflow time series prediction. *Eng. Appl. Artif. Intell.* 23, 1350–1367. doi: 10.1016/j.engappai.2010.04.003
- Zapata-Rios, X., Brooks, P. D., Troch, P. A., McIntosh, J., and Guo, Q. (2016). Influence of terrain aspect on water partitioning, vegetation structure and vegetation greening in high-elevation catchments in northern New Mexico: Terrain Aspect, Water Partitioning, Vegetation Greening in High-elevation Catchments. *Ecohydrology*. 9, 782–795. doi: 10.1002/eco.1674
- Zapata-Rios, X., McIntosh, J., Rademacher, L., Troch, P. A., Brooks, P. D., Rasmussen, C., et al. (2015). Climatic and landscape controls on water transit times and silicate mineral weathering in the critical zone. *Water Res.* 51, 6036–6051. doi: 10.1002/2015WR017018
- Zhang, Y., and Post, D. (2018). How good are hydrological models for gap-filling streamflow data? *Hydrol. Earth System Sci.* 22, 4593–4604. doi: 10.5194/hess-22-4593-2018